TÜBİTAK

Turkish Journal of Earth Sciences

http://journals.tubitak.gov.tr/earth/

Research Article

Turkish J Earth Sci
(2017) 26: 249-276

doi:10.3906/yer-1701-7

The impact of eustasy, tectonics, and paleoclimate on the dolomitization of the syn-rift Neogene carbonate platforms in the Red Sea coastal area, Egypt

Abdallah M. HASSAN*
Department of Geology, Faculty of Science, Sohag University, Sohag, Egypt

Received: 17.01.2017 • **Accepted/Published Online:** 07.07.2017 • **Final Version:** 24.08.2017

Abstract: A very significant quantity of dolomites and dolomitic limestones of variable origins occurs in the syn-rift Neogene carbonate platforms of the NW Red Sea coast and the Gulf of Suez**.** These are more common in the Um Diheisi Member of the Ranga Formation (early Miocene), the Um Mahara Formation (middle Miocene), the Um Gheig Formation (late Miocene), and the Dashet El Dabaa Member of the Shagra Formation (Pliocene). Based on their stratigraphic distribution, petrography, and cathodoluminescent characteristics, as supported by geochemical data, syn-rift irregular morphotectonic relief, and the eustasy, four distinct types of dolomites have been identified and were interpreted as follows: 1) Syndepositional stratiform dolomicrite of the Um Diheisi Member occurred in structurally half graben restricted basins favoring structural sites of cyclic peritidal dolomitization that developed in response to sea transgression and then short-term sea level fall of each cycle period. 2) Regional replacive dolomite of the Um Mahara Formation involved mixing meteoric, marine, and hypersaline waters associated with the highstand sea level and then the repeated emergence of the platform and the temporal drowning with restricted marine waters. 3) Mixed syndepositional, replacive, and void-filling cement dolomites of the Um Gheig Formation, which suggest three dolomitization events:- i- an early, penecontemporaneous dolomite associated with highstand phases; ii- diagenetic dolomites formed by mixing meteoric and hypersaline reflux waters during lowstands and falling sea level, and iii- the latest dolomitization phase that occurred as dolomite cement involving hydrothermal fluids during the exposure periods. 4) Replacive dolomite of the Dashet El Dabaa Member, which involved mixtures of hypersaline and marine waters. Paleoclimate played an important role in the dolomitization of the Neogene sediments. An arid climate prevailed during the dolomite of the Um Diheisi Member and the early dolomitization phases of the Um Gheig Formation. A humid climate predominated in the replacive dolomite of the Um Mahara Formation, in which the meteoric groundwater allowed the dissolution of precursor limestones and subsequent formation of extensive bodies of dolomites. Arid conditions also prevailed during the dolomitization of the Dashet El Dabaa Member, as evidenced by the lack of dissolution and the abundance of well-preserved unstable feldspars.

Key words: Dolomitization, cathodoluminescence, mixing zone, penecontemporaneous, peritidal, stable isotopes, hypersaline

1. Introduction

Various models have been proposed to account for the process of dolomitization. Several of the popular models for dolomitization are penecontemporaneous or very early diagenetic and near-surface processes. In recent years various dolomitization models have been tied into the concepts of sequence stratigraphy (Gorody, 1980; Jadoul et al., 1991; Van den Hurk and Betzler, 1991; Montanez and Read, 1992; Tucker et al., 1991; Tucker, 1993; Mresah, 1998; Haas and Demeny, 2002; Teedumae et al., 2004; Turhan et al., 2004; Schwarzacher, 2005). Montanez and Read (1992) and Turhan et al. (2004) suggested that the fluctuating sea level exhibits the lateral progradation of carbonate platforms and development of a wide flat surface leading to formation of extensive dolomites by brines or mixed dolomitizing waters. Tucker (1993) and Mresah (1998) mentioned that the pervasive dolomite in the carbonate platforms is formed by lateral migration of the dolomitizing fluid during periods of relative sea level oscillations, especially associated with regressive phases of sea level (Teedumae et al., 2004). On the other hand, some authors (e.g., Iannace and Frisia, 1991; Bosence et al., 2000; Soreghan et al., 2000; Haas and Demeny, 2002) mentioned that the early dolomitization of the platform carbonates was controlled by climate and high-frequency sea level oscillations.

In the NW Red Sea and Gulf of Suez area, dolomitization is considered one of the major and largest diagenetic processes that affected the Neogene carbonate platforms. This phenomenon was dealt with by some authors, most of them focusing on middle Miocene dolomitization of certain areas along the NW Red Sea and the Gulf of Suez

* Correspondence: geoabdallah@yandex.com

(e.g., Aissaoui et al., 1986; Coniglio et al., 1988; Sun, 1992; Shaaban et al., 1997; Clegg et al., 1998). Other studies dealt with the problem in a general manner (e.g., Purser, 1998; El-Haddad, 2004). Coniglio et al. (1988) mentioned that dolomitization of the middle Miocene carbonates at the Abu Shaar area was related to the mixing of two waters, meteoric and marine waters, while Sun (1992) and Clegg et al. (1998) suggested that the mixing of four types of waters, meteoric, normal marine, hypersaline, and hydrothermal, was involved in dolomitization processes. Purser (1998) believed in heated basinal sea waters for dolomitization, whereas El-Haddad (2004) believed in the mixing of meteoric water and sea water together with formation water in the rocks for the regional dolomitization of the middle Miocene carbonates in the Red Sea, which was extensively active during the evaporative sea level drawdown. On the other hand, Shaaban et al. (1997), in their work at the Um Gheig area, suggested that the middle Miocene dolomitization took place within a zone of circulating marine pore fluids ahead of a mixing zone.

All the previously mentioned studies dealt with the dolomitization of the preevaporite middle Miocene carbonates, whereas no studies are known on the dolomitization of the early and late Miocene and Pliocene carbonates, especially when most of these carbonates include early and epigenetic dolomites. Furthermore, no studies have been carried out on the environment of the dolomite formation and its relationship to sea level fluctuations, rift tectonics, and paleoclimatic conditions.

The aim of this paper is to study the regional distribution, environment, and origin of the penecontemporaneous and epigenetic Neogene dolomites and to propose dolomitization models in view of the sea level oscillations, rift tectonics, and paleoclimate.

2. Stratigraphic outline

The Neogene stratigraphy of the Egyptian Red Sea coastal area has been discussed by many authors (e.g., Akkad and Dardir, 1966; Issawi et al., 1971; Samuel and Saleeb-Roufaiel, 1977; Montenant et al., 1988; Purser et al., 1990; Philobbos et al., 1989, 1993). The Neogene sequence is dominated by mixed carbonate and siliciclastic rocks that have been deposited in a basin whose origin is related to rifting processes (Purser et al., 1987). Due to repeated tectonic events, the syn-rift sequence is characterized by numerous spectacular rapid vertical and lateral changes in thicknesses and facies. A brief lithologic description of the Neogene sequence, from oldest to youngest, is given below:

1) The Abu Ghusun Formation (Oligocene?): The Abu Ghusun Formation (Philobbos et al., 1988) unconformably overlies the basement rocks and underlies the Ranga Formation. It is composed of about 40 m of red and brick-red conglomeratic sandstones, sandstones, siltstones, and claystones.

2) The Ranga Formation (early Miocene): The Ranga Formation (45 m, Samuel and Saleeb-Roufaiel, 1977) unconformably overlies and cuts through the Abu Ghusun Formation. It consists of three synchronous members interfingering with each other. These are given (Philobbos et al., 1993) the following formal names: Um Abas (conglomerate) Member, Um Diheisi (carbonate) Member, and Rosa (evaporite) Member.

3) The Um Mahara Formation (middle Miocene): The Um Mahara Formation (Samuel and Saleeb-Roufaiel, 1977) overlies the Ranga Formation and/or the basement rocks. Generally, the Um Mahara Formation is subdivided into two parts: a lower part of reefal carbonates and mixed siliciclastics-carbonates (total thickness: 10–50 m), and an upper part of mixed siliciclastics and algal laminated carbonates (40–80 m).

4) The Abu Dabbab Formation (middle-late Miocene?): The Abu Dabbab Formation (Akkad and Dardir, 1966) discordantly overlies the Um Mahara Formation and is composed mainly of massive anhydrite with minor gypsum and halite (total thickness 80 m).

5) The Um Gheig Formation (upper Miocene): The Um Gheig Formation (Samuel and Saleeb-Roufaiel, 1977; Philobbos and El Haddad, 1983a, 1983b) conformably overlies the Abu Dabbab Formation. It is represented by either hard crystalline bedded carbonate or highly weathered brown dolomitic limestone (15–20 m).

6) The Marsa Alam Formation (Mio-Pliocene): The Marsa Alam Formation (Philobbos et al., 1989) conformably overlies the Abu Dabbab Formation and is distinguished into three members: a lower Samh Member (upper Miocene?) composed of fine siliciclastics 30 m thick (siltstones, claystones, and sandstones); the Gabir Member (Pliocene), represented by dominantly siliciclastic and bioclastic-oolitic limestone (40–60 m); and an upper Abu Shegeili Member (Pliocene) composed of a conglomeratic sequence (total thickness 20–50 m).

7) The Shagra Formation (Pliocene): The sediments of the Shagra Formation (Akkad and Dardir, 1966) are composed of two parts (Philobbos and El Haddad, 1983a, 1983b): a lower mixed siliciclastic-carbonates sequence (Dashet El Dabaa Member, 20 m thick) and an upper dominantly carbonate sequence (Sharm El Arab Member, 40 m thick). It is noticed that the Shagra Formation clearly interfingers with the Abu Shegeili Member.

8) The Samadai Formation (Plio-Pleistocene): The Samadai Formation (Philobbos et al., 1989) is composed of coarse siliciclastics and mixed siliciclastic-carbonate sequences (total thickness 100 m), which unconformably overlies a beveled surface of the underlying Marsa Alam Formation.

3. Materials and methods

Nine localities along the NW Red Sea coast and Gulf of Suez were chosen for dolomite investigation. These are: west of Ras Honkorab, Wadi El Gemal, Sharm El Bahari-Sharm El Qibli, Um Gheig, Gabal Gazerat El-Hamra, Gabal Abu Shegeili El Bahari, Wadi Ambagi, Ras Samadai, and Gabal Gharamoul (Figure 1). For sequence stratigraphic interpretation and dolomitization investigation, 25 vertical sections were measured in the Neogene formations, where lithofacies variations and sequence boundaries in different tectonic situations were observed. About 200 thin sections were cut in the collected samples, and all were stained with Alizarin Red S and potassium ferricyanide solution to differentiate calcite, ferroan dolomite, and dolomite, using the method of Dickson (1966). Thin sections were examined using a polarizing microscope in order to study the dolomite petrography. Representative samples were also studied using cathodoluminescence with a Technosyn cold-cathode luminoscope, Model 8200 MK II, in the laboratories of the Institute of Geology and Paleontology at the University of Innsbruck, Austria. The petrographic characteristics and diagenetic features as well as episodes of dolomitization were recognized using petrographic techniques and cathodoluminescence techniques.

Geochemical analysis of bulk samples concentrated on major and trace elements, carbon and oxygen stable isotopes, and X-ray powder diffraction. Twenty-three representative samples were further analyzed for their major (CaO and MgO) and trace (Na^{+}, Sr^{+2}, Mn^{+2}, Fe^{+2}, K^{+}, and Ba^{+2}) element contents by inductively coupled argon plasma emission spectroscopy (ICAP-OES, PU 7000) in the Innsbruck Laboratory, Austria (Table 1). Fifty bulk samples were analyzed in the same laboratory by X-ray diffraction, using a Phillips PW 1170 X-ray diffractometer to determine the mineralogy.

For stable carbon and oxygen isotopes analyses, 12 bulk carbonate samples were reacted with 100% phosphoric acid at 75 °C in an online carbonate preparation system attached to a Finnigan Mat 252 mass spectrometer. All values are reported in per mill relative to the V-PDB by assigning $\delta^{13}C$ value of +1.95 and $\delta^{18}O$ value of –2.20 to NBS-19. Oxygen isotopic composition of the dolomites was corrected using the fraction factors given by Rosenbaum and Sheppard (1986). The carbon and oxygen isotopes of

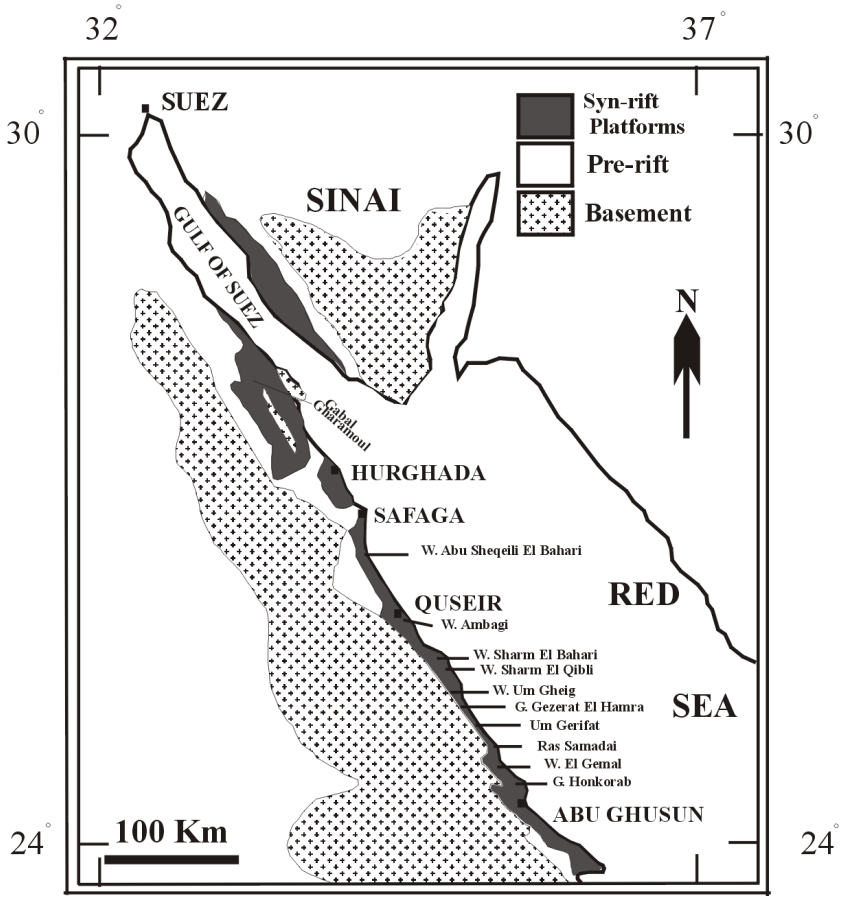

Figure 1. Location map of the studied localities.

Table 1. Major and trace elements in representative samples of the different Neogene dolomites.

1- Um Diheisi dolomites											
Major oxides (%)					Trace elements (ppm)						
Samp. No.	CaO	MgO	SiO_2	Al_2O_3	Fe	Mn	K	P	Ba	Sr	Na
4 Dh	29.64	21.84	3.11	0.69	6910	694	971	1788	43	186	831
6 Dh	29.54	21.87	1.35	0.784	4525	946	1004	2097	76	167	1187
12 Dh	29.04	21.46	6.14	1.64	8392	1370	2872	2237	110	234	1342
8 Sm	30.29	19.38	0.66	0.29	2734	1838	207	2749	42	73	504
16 Sm	29.13	21.06	1.21	0.36	1133	423	323	1538	54	88	543
2- Um Mahara dolomite											
Samp. No.	CaO	MgO	SiO_2	Al_2O_3	Fe	Mn	K	P	Ba	Sr	Na
1 Sh	30.14	20.86	3.32	1.01	5007	3767	1311	1035	214	298	675
7 Sh	29.24	21.26	3.69	0.79	5462	1649	1843	792	21	539	289
13 Sh	30.55	21.23	1.27	0.19	1993	1144	132	586	75	413	378
18 Sh	29.18	21.09	2.85	0.57	5168	1947	1203	1626	12	367	586
19 Sh	29.31	19.75	3.36	0.78	8063	3757	1203	252	32	198	600
3- Um Gheig dolomites											
Samp. No.	CaO	MgO	SiO_2	Al_2O_3	Fe	Mn	K	P	Ba	Sr	Na
1 Um	31.06	20.66	0.36	0.2	800	3500	230	230	64	356	700
2 Um	31.04	20.62	0.3	0.16	2000	3566	270	250	29	337	500
3 Um	32.73	18.11	0.3	0.25	3000	2228	250	244	23	364	550
1 m	29.94	21.08	0.37	0.041	3916	2028	41	244	21	421	527
4 m	30.29	21.68	0.12	0.028	2028	8698	116	58	23	143	527
8 m	29.91	21.23	0.48	0.13	1140	4227	74	757	94	495	386
15 m	30.17	21.93	0.16	0.04	804	4876	58	58	21	153	356
4- Dashet El Dabaa dolomite											
Samp. No.	CaO	MgO	SiO_2	Al_2O_3	Fe	Mn	K	P	Ba	Sr	Na
5 Ug	29.66	19.82	1.86	0.42	2566	209	332	233	10	140	890
8 Ug	27.63	19.32	19.5	2.3	3049	192	5055	314	100	190	4050
9 Ug	30.61	19.63	1.83	0.5	2363	219	572	355	10	20	853
10 Ug	30.02	10.39	5.05	0.7	2342	109	1311	337	30	230	6847
11 Ug	30.22	19.67	2.87	0.54	1692	109	963	58	30	230	4510
12 Ug	30.06	19.04	3.81	0.59	2349	166	1170	215	30	250	2529

dolomites were analyzed at the University of Erlangen, Germany.

4. Dolomite characteristics and environments

The sequences comprising dolomite and dolomitic limestones are more common in the Um Diheisi Member of the Ranga Formation (early Miocene), the Um Mahara Formation (middle Miocene), the Um Gheig Formation (late Miocene), and the Dashet El-Dabaa Member of the Shagra Formation (Pliocene, Figure 2).

4.1. Dolomites of the Um Diheisi Member of the Ranga Formation (early Miocene)

4.1.1. Petrography and geochemistry

The Um Diheisi dolomite representing the earliest Neogene dolomitization is limited to structurally controlled half grabens (e.g., Gabal Ras Honkorab and Wadi Um Gheig). It unconformably overlies either the pre-rift sedimentary cover or the basement (Figures 3A, 3B, 4A, and 4B). Laterally and downwards it interfingers

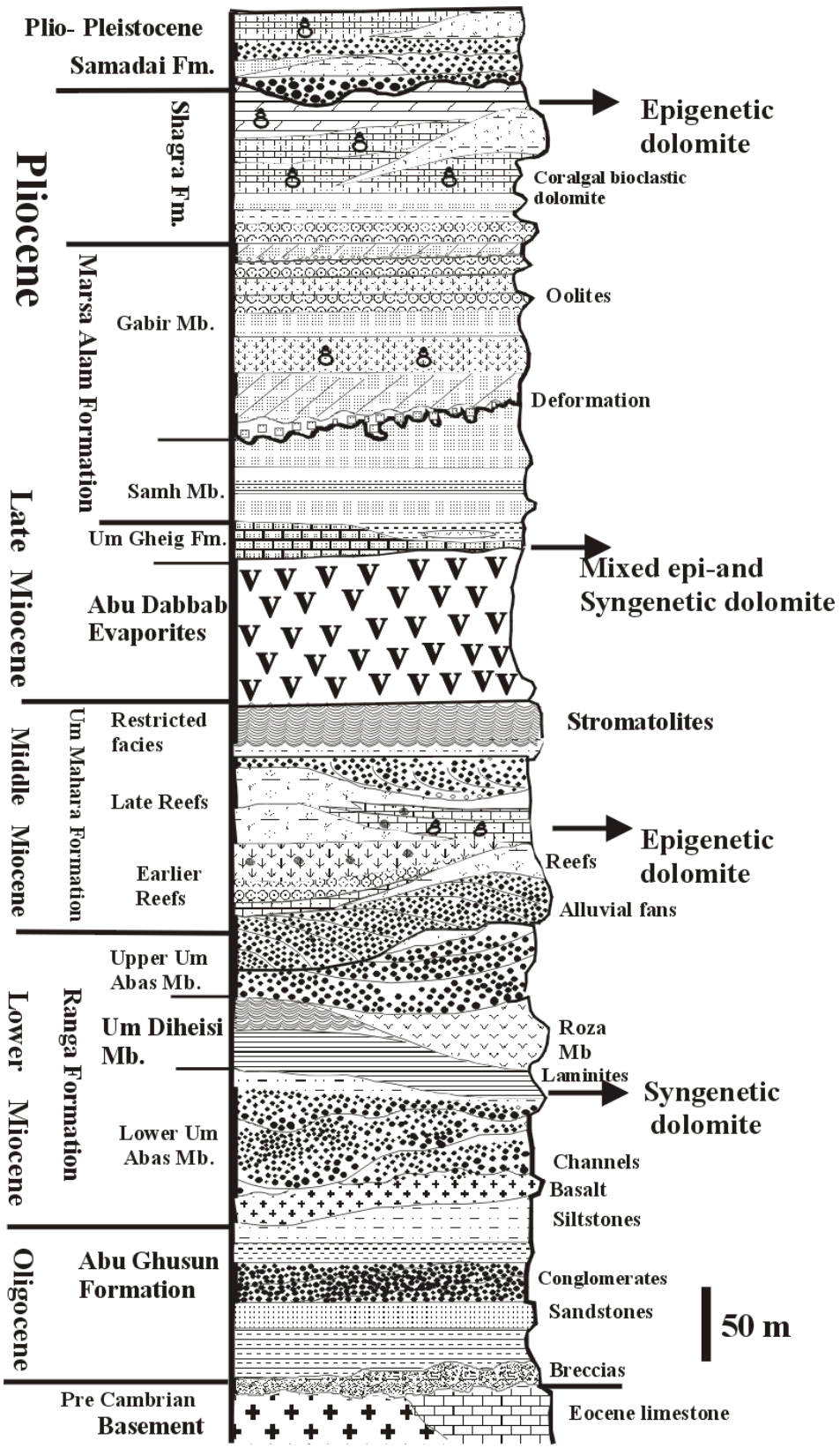

Figure 2. Generalized stratigraphic Neogene sequence of the NW Red Sea, showing the location of dolomitization. For the stratigraphic nomenclature, see the text.

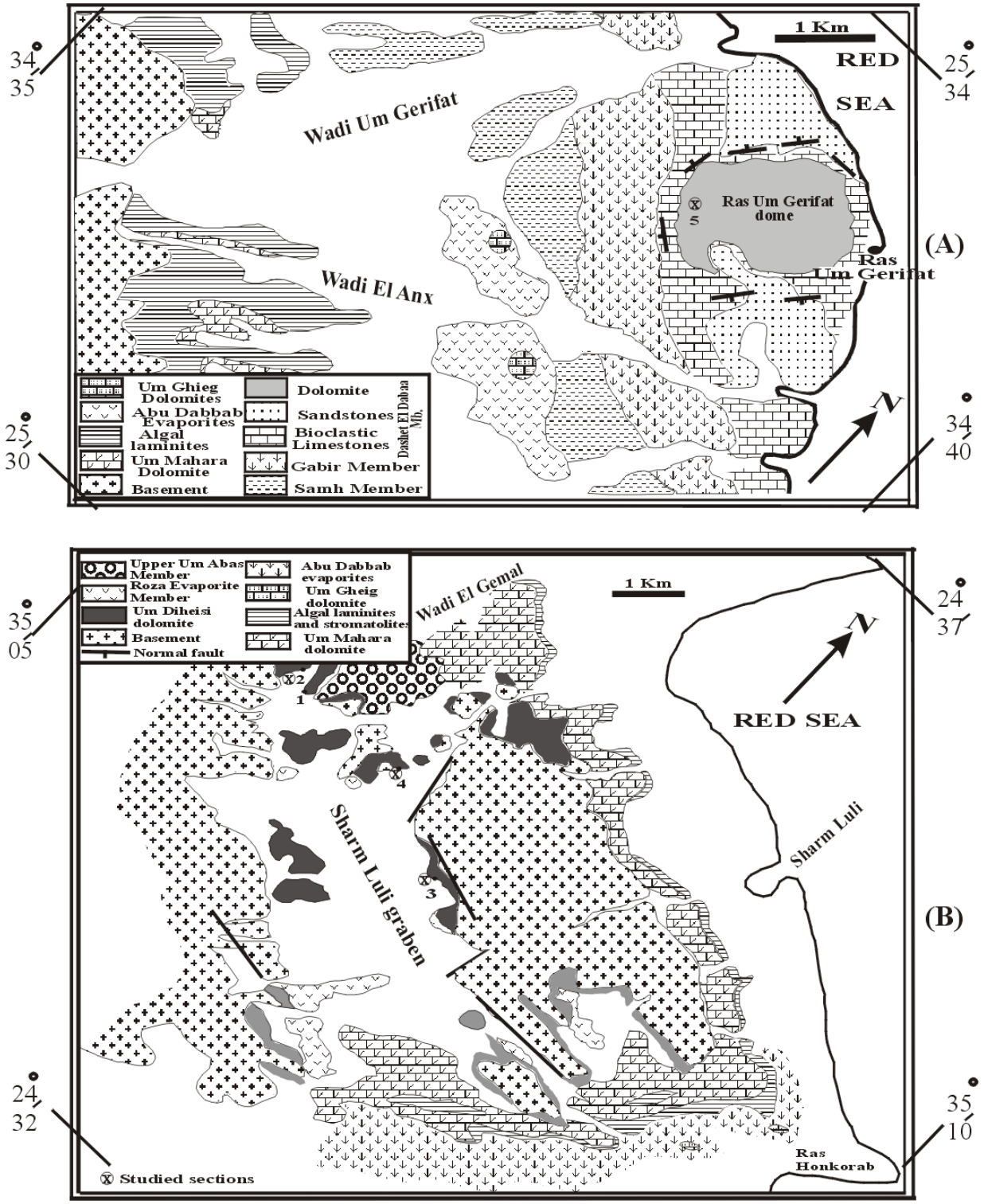

Figure 3. Simplified geological maps of the studied areas: A) Ras Um Gerifat area showing the distribution of early and late Neogene dolomites, B) area north of Ras Honkorab showing the distribution of the early Neogene dolomites.

with the Roza Evaporite Member in low-lying areas (Figure 4C). In depressions, the sequence is composed of 20-m-thick vertically repeated 8-m-thick shallowing upward peritidal dolomite cycles. Laterally, towards fault scarps and crests of blocks, the sequence merges into three cycles (up to 4 m thick each). The cycles are dominantly dolomite, each starting with intertidal brecciated, vuggy dolomite, followed upward with regressive intertidal facies composed of algal laminites with fenestrae. Supratidal algal stromatolites and laminites facies represent the peak of the shallowing-upward trend observed in the upper part of each cycle (Figures 4D and 4E). Fossils are scarce, while bird's eye fabric and intraclasts are common (Figure 4F). In the depressions, the basal part of the lower cycles is dominated by subtidal micritic limestones and mudstones. In this situation the degree of dolomitization increases upwards, indicating a close genetic relationship between the depositional environment and dolomitization.

Petrographically, the dolomite is brownish to grayish yellow in color and has crystals ranging in size from 3 to 45 μm, and it shows a mosaic texture (Figure 4G). Strata proximal to sequence boundaries exhibit coarse-grained dolomite crystals (up to 100 μm). Some original fabrics show dissolution cavities of preexisting evaporite minerals (Figure 4H). The cathodoluminescence of the dolomite crystals is dull to uniformly dark brown and unzoned.

The dolomite cycles contain horizons showing evidence of prolonged subaerial exposure in the form of dissolution and pedogenesis, which took place by the end of each short-term sea level fall. The cycles are bounded by disconformities as a rule and best developed in cycles situated on crests of tilted blocks and their fault scarps (Figure 5).

Oxygen isotope values (Table 2) exhibit a range from 1.17‰ to –1.24‰ PDB, while $\delta^{13}C$ shows a range of variation between –6.88‰ and –7.40‰ PDB (Figure 6). A progressive increase in Fe^{+2} and Mn^{+2} concentrations is observed in the upper part of this dolomite, where their values range from 694 ppm to 8392 ppm.

X-ray diffraction (Figure 7) indicates that samples are either pure (100%) dolomite or dolomite with calcite, palygorskite, and some traces of anorthite. The Sr^{+2} content of dolomites of Um Diheisi ranges from 160 ppm to 295 ppm (Table 1). However, some stromatolitic samples at the top of the Um Diheisi dolomite have relatively low Sr^{+2} content (up to 80 ppm). Na^{+} concentration varies from 504 ppm to 1342 ppm. Ba^{+2} content varies from 7 ppm to 169 ppm.

4.1.2. Environment and origin of dolomite formation

The preservation of original fabrics such as the cryptalgal laminites and stromatolites, in addition to the abundance of dissolution cavities of preexisting evaporite minerals, indicate that dolomite of the Um Diheisi Member was formed in an early stage by hypersaline sea water concentrated in restricted peritidal environments synchronous with tidal deposition. It very possibly documents lowstand basin restriction (Qing et al., 2001; Hass and Demeny, 2002; Teedumae et al., 2004). The peritidal shallowing-upward sequences with rhythmic sedimentation have been mostly interpreted as a consequence of autocyclic and progradation mechanisms. Kuznetsov (1991) mentioned that the peritidal zone has geochemical conditions for enhanced magnesium compound precipitation. Similar dolomite is forming today in numerous Holocene peritidal environments (Zenger and Dunham, 1988). The presence of desiccation cracks, reworked polygons, intraclasts, and planar, irregular fenestrae as well as bird's eye structures confirm peritidal facies. Similar observations were recorded in the peritidal dolostones in the Ordos area of North China (Zengzhao et al., 1998) and in Lea County, New Mexico (Zenger and Dunham, 1988). The presence of arkosic quartz sands associated with supratidal facies is interpreted to have been deposited by aeolian processes during repeated subaerial exposures. This is consistent with the presence of horizons showing dissolution, pedogenesis, and dedolomitization by the end of each cycle, an observation that was also recorded earlier by Khalifa and Abu El-Hassan (1993).

The penecontemporaneous origin of the Um Diheisi dolomite is documented by the presence of fine crystalline texture (Qing et al., 2001). This suggests that the Um Diheisi dolomite crystallized rapidly, being consistent with dolomitization by hypersaline sea water in a peritidal setting. Zengzhao et al. (1998) mentioned that tidal flat dolomite is dominated by fine-grained crystal sizes. No recognizable fossils were found in any of these dolomite types. Such a situation could result in penecontemporaneous dolomitization, because the hypersalinity enhancing dolomitization could have stifled faunas. This is documented by a good preservation of unstable feldspar grains (anorthite) in some samples, indicating that no significant amount of surface meteoric waters passed through the initial dolomitization process. The presence of palygorskite associated with the Um Diheisi dolomite documents that dolomitization took place in a closed hypersaline supratidal setting. This interpretation is consistent with that of Velde (1992) and El-Shater and Philobbos (1998), who mentioned that the palygorskite was formed in supratidal lagoonal and sabkha environments. The petrographic luminescence indicates that the Um Diheisi dolomite occurs as nonluminescent, dull to brown unzoned crystals and is consistent with the initiation of dolomite growth in hypersaline water.

The Na^{+} content varies from 504 to 1187 ppm, similar to values of ancient supratidal dolomites described by Baum et al. (1985) and also comparable to those of Holocene hypersaline dolomites (Land and Hoops, 1973). This

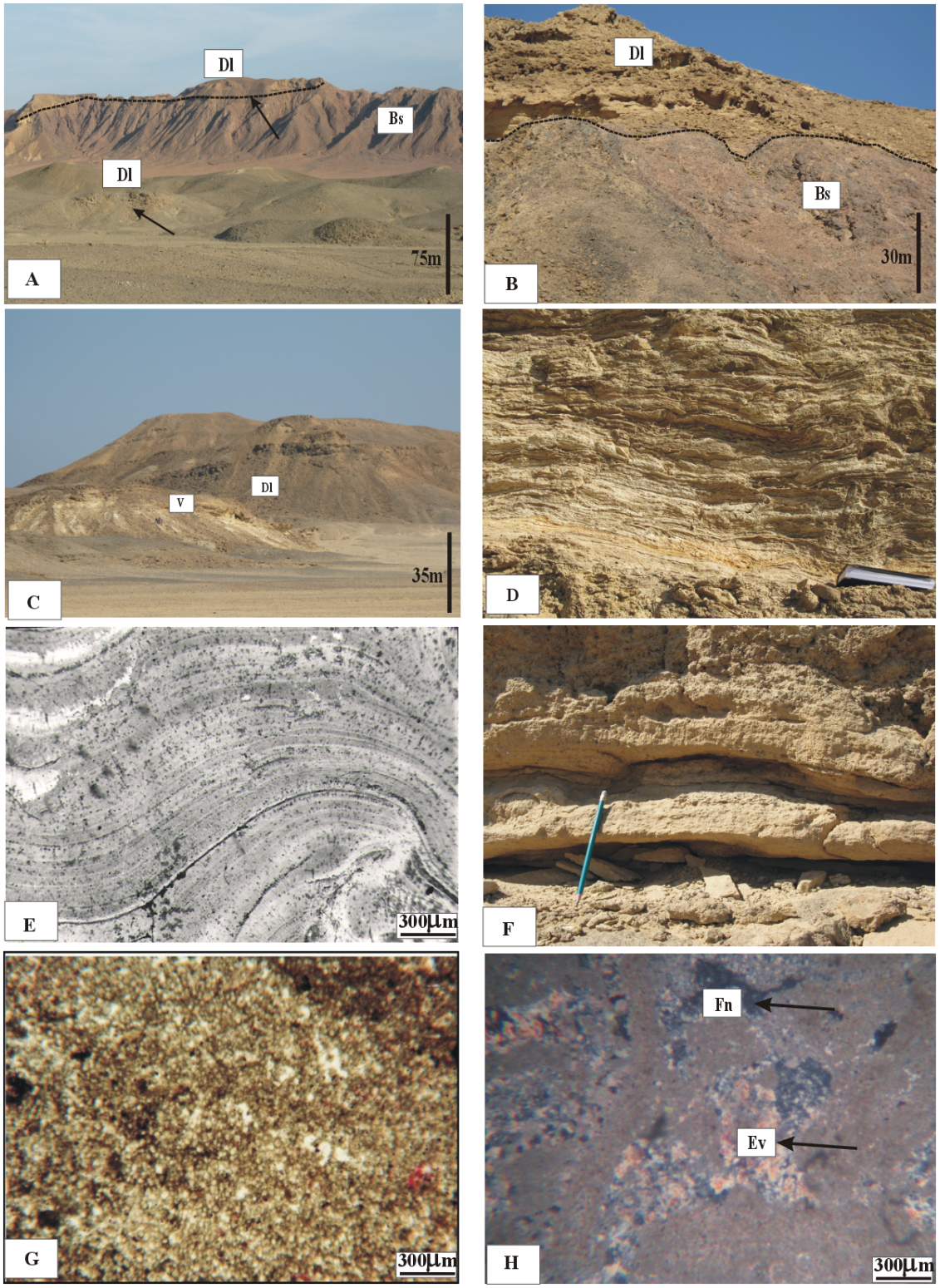

Figure 4. A) Field photograph showing Um Dihiesi dolomite (Dl) occurring on basement fault scarps (Bs), crests of blocks, and in structural depressions; B) close-up view showing the dolomite overlying the basement rocks; C) Roza evaporate (V) interfingering with dolomite (Dl) in low-lying areas; D) close-up view of algally laminated dolostones; E) photomicrograph of stromatolitic dolomicrite; F) field view of algal laminated stratiform dolomite with bird's eye structures; G) photomicrograph of microcrystalline dolomite; H) photomicrograph of fine dolomite with fenestrae (Fn) and evaporite minerals (Ev).

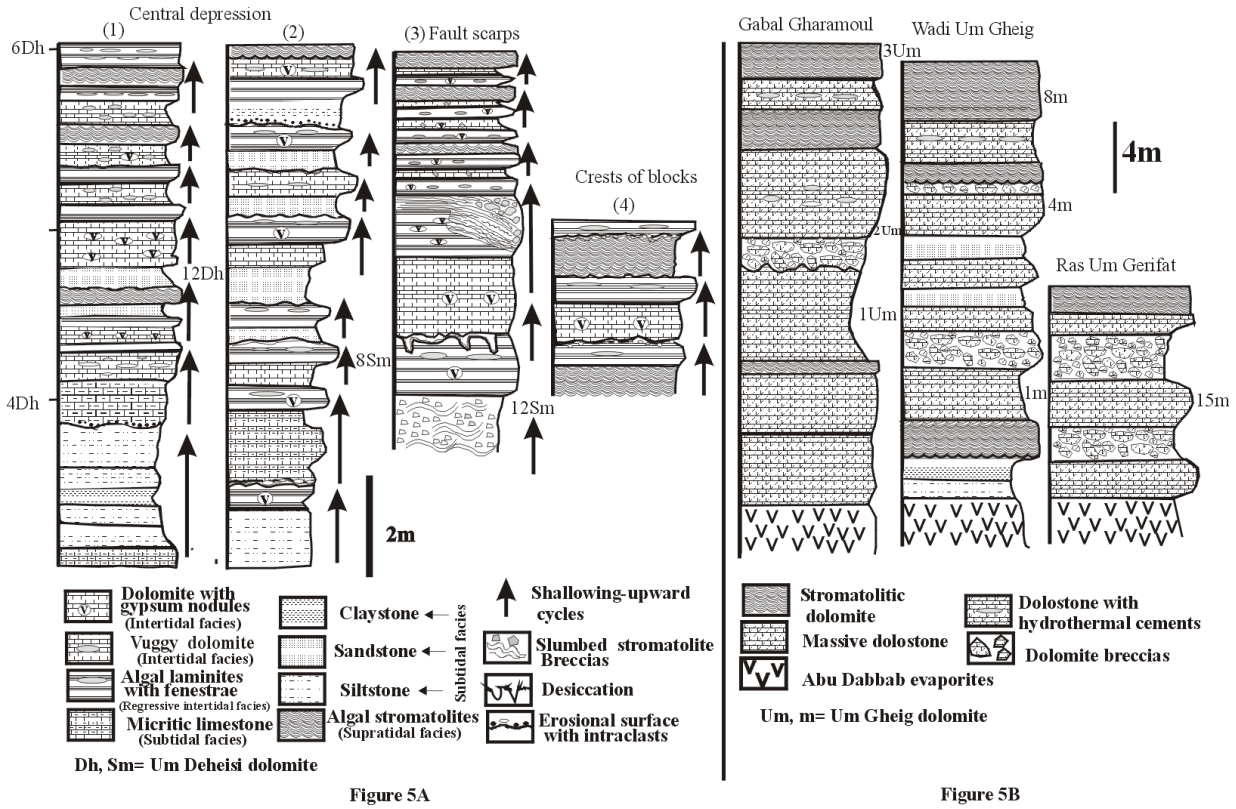

Figure 5. A) Representative measured sections of the Um Diheisi dolomite; for location, see Figure 3. B) Representative measured sections of the Um Gheig dolomite; for location, see Figure 1.

Table 2. Stable isotope composition of the Neogene dolostones.

Formation	Samp. No.	$\delta^{18}O$ (‰ PDB)	$\delta^{13}C$ (‰ PDB)
Um Diheisi dolomite	4 Dh	1.17	–6.88
	8 Sm	–1.24	–7.4
Um Mahara dolomite	7 Sh	–4.52	–5.84
	18 Sh	–4.34	–5.96
	13 Sh	–1.38	–0.91
Um Gheig dolomite	7 m	–3.94	–9.84
	15 m	–3.99	–8.72
	5 As	–7.81	–10.07
	2 G	–5.32	–7.72
	8 G	–5.87	–6.91
Dashet El-Dabaa dolomite	9 Ug	2.66	–10.86
	12 Ug	3.23	–13.03

suggests that the Um Diheisi dolomite was possibly formed from fluids with Na^{+} ratios similar to modern hypersaline water. Locally, in samples on footwall blocks, Na^{+} and Sr^{+2} concentrations have the lowest values, being consistent with the general depletion of Ba^{+2} content, a phenomenon that clearly indicates extensive depletion by meteoric groundwater throughout the prolonged emergence of the cycles. This interpretation is in accordance with that of Balog et al. (1999), who noted that in Triassic peritidal dolomites, Sr^{+2} and Na^{+} underwent depletion by meteoric

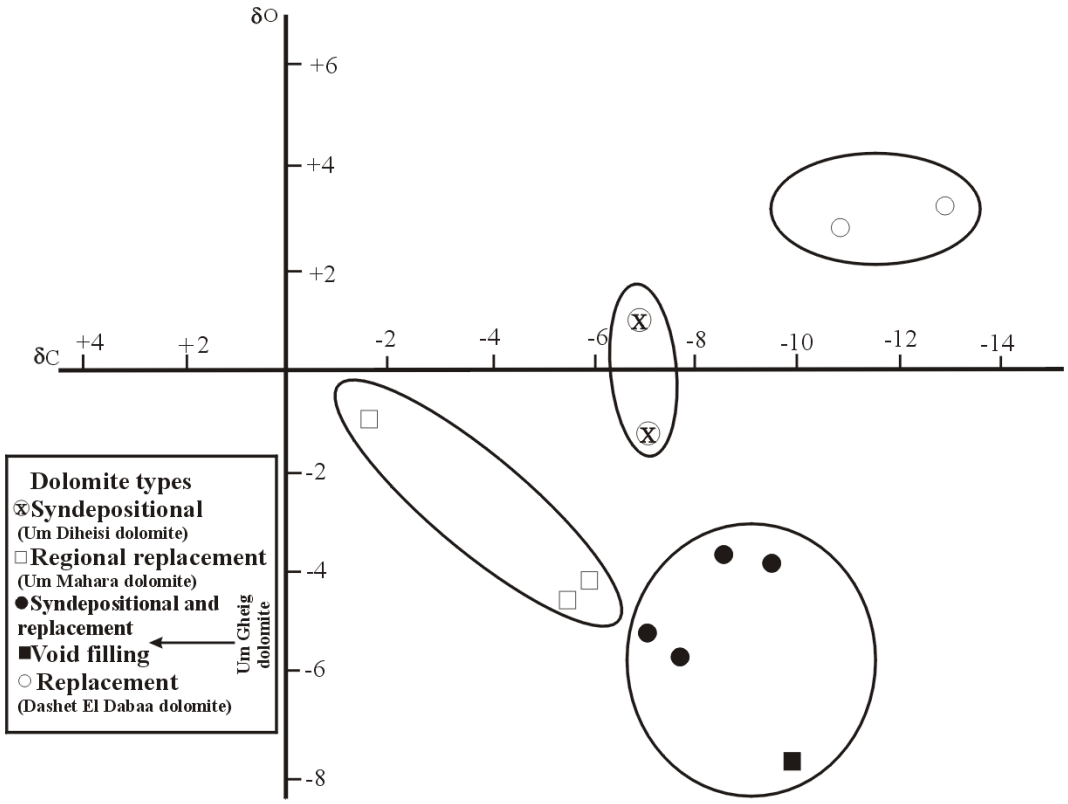

Figure 6. Cross-plot of oxygen and carbon isotopic composition of the Neogene dolomites of the NW Red Sea and Gulf of Suez.

influences. The relative increase of Mn^{+2} and Fe^{+2} may be interpreted according to the opinion of Veizer (1983) such that these trace elements tend to be enriched in dolomites from saline waters.

The positive oxygen isotope values document that hypersaline sea water has been involved, similar to the other ancient penecontemporaneous dolostones (Moore, 1989; Tucker and Wright, 1990). The common negative $\delta^{13}C$ values (Table 2) of this dolostone may reflect the presence of organic matter and bloom of microbial productivity accumulated at the water–sediment interface (Nedelec et al., 2007).

4.2. Dolomites of the Um Mahara Formation (middle Miocene)

4.2.1. Petrography and geochemistry

According to facies characteristics and the environment of deposition, the Um Mahara Formation is subdivided into early platform facies composed of open marine mixed siliciclastics and carbonates showing a progradation nature (Figure 8A), followed upwards with a late platform restricted marine algally laminated and stromatolitic carbonate facies (Figure 8B; El-Haddad et al., 1984; Mahran et al., 2007). The early platform and the associated talus are extensively dolomitized over a much larger region.

Petrographically, the Um Mahara dolomite occurs as a replacement of both cement and some allochems and as void-filling resulting from the dissolution of aragonitic bioclasts and reef frame, either before or during dolomitization. The replacement type has a general cloudy appearance under plane-polarized transmitted light and is fabric-destructive, similar to replacive dolostones described by Nicolaides (1995). Three types of dolomites have been distinguished based on morphology and crystal size: i- microdolomite (10 μm to 30 μm), which mimetically replaced the precursor limestone cements and red algal and mollusks, similar to fine crystalline dolomite in South-Central Saskatchewan, Canada (Qilong et al., 2007); ii- euhedral, mosaic dolomite (100 μm); and iii- coarse multiple zoned dolomites exhibiting alternations of dark and clear rims (varying from 200 μm to 300 μm in size, Figures 8C and 8D). Aragonitic bioclasts including corals have been completely dolomitized, whereas other bioclasts of high-magnesium calcite like coralline algae are preserved, despite the complete replacement of the cement by dolomite. Preservation is so perfect that the cellular structure is retained (Figures 8E and 8F). Occasionally a small proportion of bioclasts is still partially preserved as calcite. Under cathodoluminescence, the Um Mahara

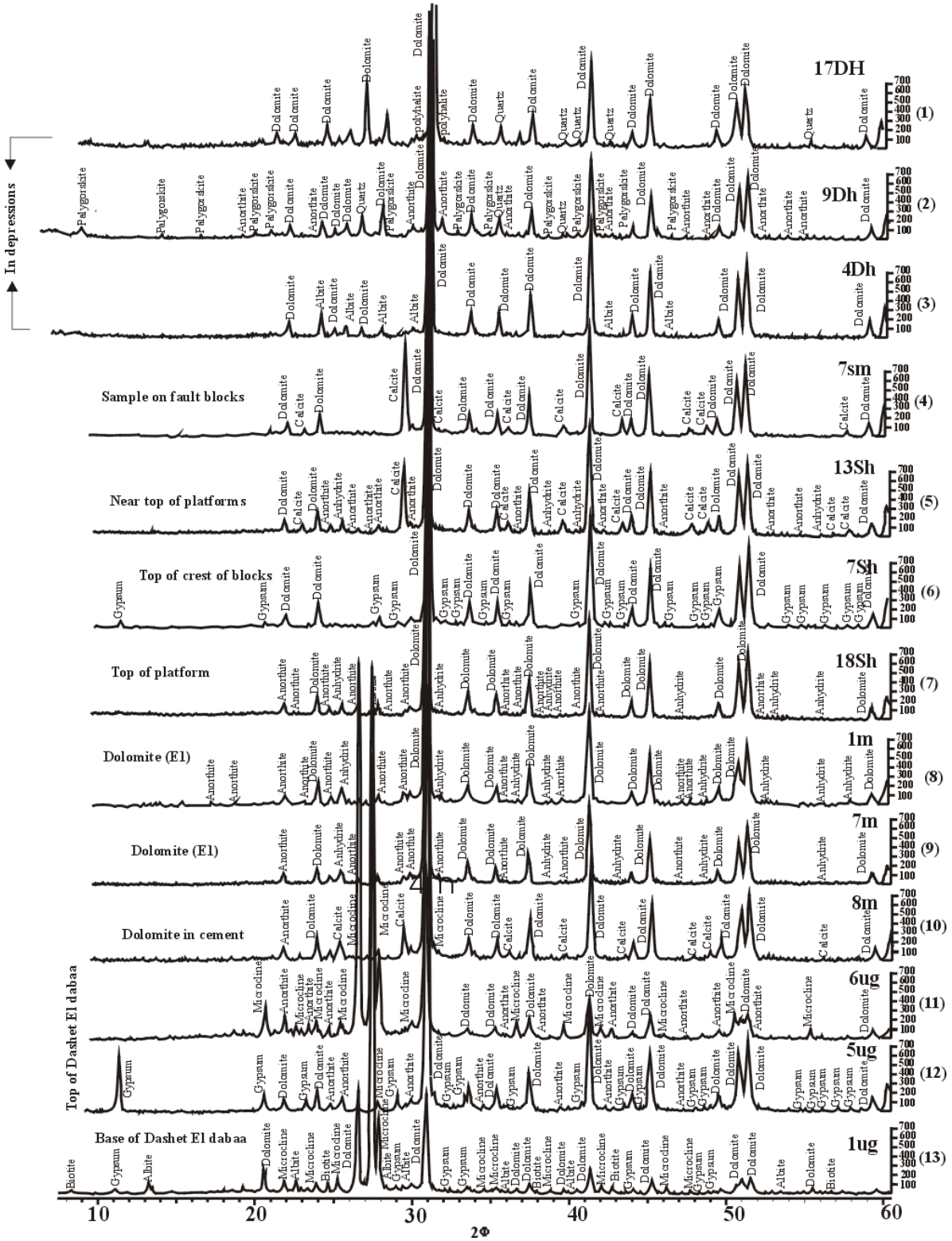

Figure 7. X-ray diffraction pattern of representative powdered samples from the different Neogene dolomite formations, 1–4 = Um Deheisi dolomite, 5–7 = Um Mahara dolomite, 8–10 = Um Gheig dolomite, 11–13 = Dashet El-Dabaa dolomite.

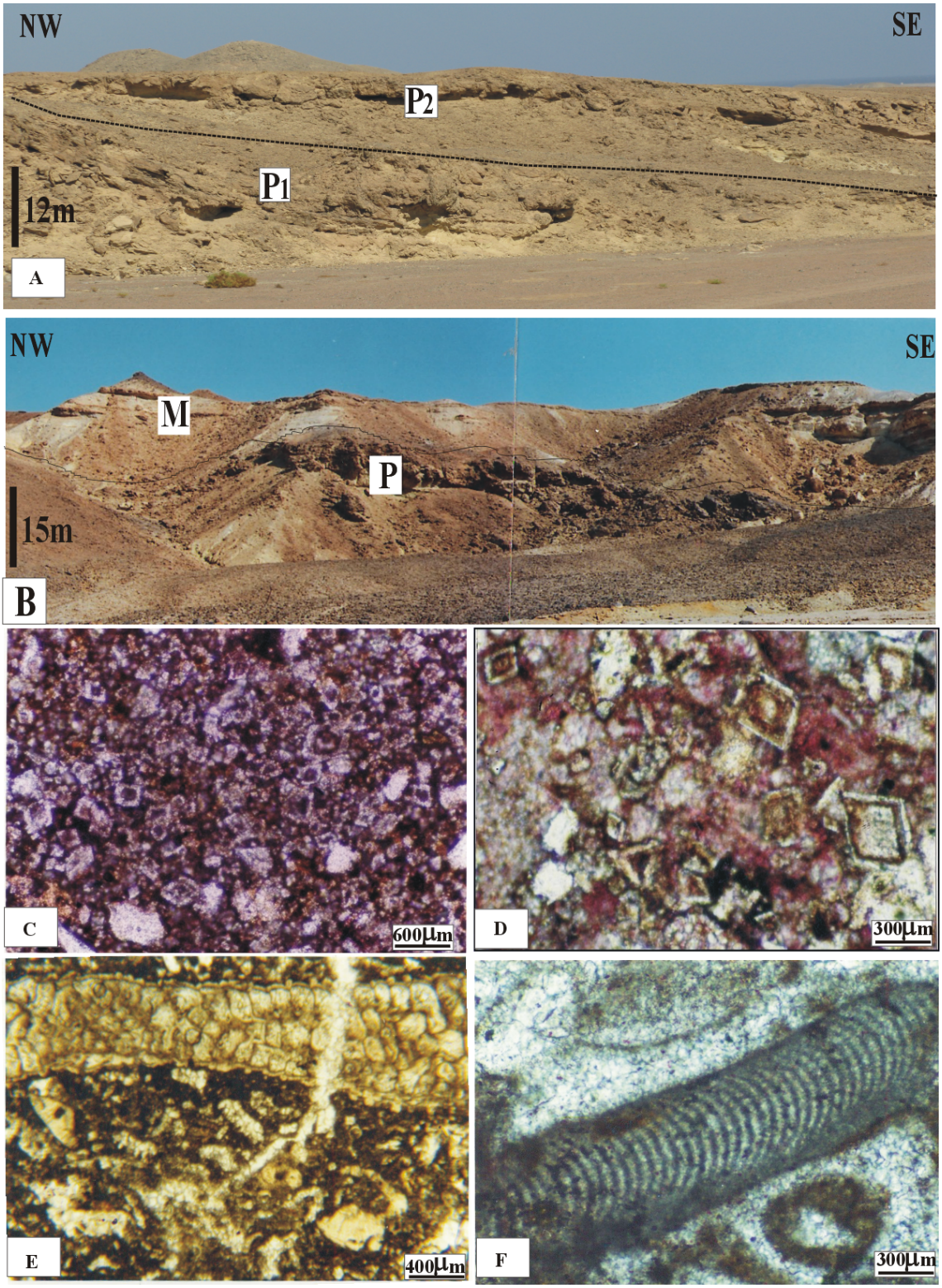

Figure 8. A) NW-SE panorama showing the progradation nature of Um Mahara dolomite, north Wadi El-Gemal, where the dashed line separates two prograding carbonate bodies (P1 & P2); B) NW-SE panorama showing the earlier progradation dolomite (P), onlapped by restricted marine facies (M), Wadi Sharm El-Qibli; C) photomicrograph of Fe-zoned dolomite crystals, west of Ras Honkorab; D) close-up view of the dolomite rhombs in 8C showing interrhombic cement; E) mimetic dolomite of bryozoan forams; F) preservation of the cellular structure of coralline algae despite complete replacement of matrix by microsparitic dolomite.

dolomites have relatively uniform, moderately reddish orange color with occasional dull zoning.

Geochemically, the Um Mahara dolomite exhibits a range of $\delta^{18}O$ (PDB) values from –1.38‰ to –4.52‰. Mean δ^{13} C ranges from –0.91‰ to –5.96‰ (Table 2). X-ray diffraction indicates that samples are of either pure (100%) dolomite or dolomite with calcite, gypsum, and anhydrite. The concentration of Na^{+} in the dolomitized Um Mahara Formation varies from 289 ppm to 675 ppm (see Table 1). Its Sr^{+2} content varies from 198 ppm to 413 ppm, falling within the estimated Sr^{+2} content range for the middle Miocene dolomites of Abu Shaar, west of the Gulf of Suez (Coniglio et al., 1988). Fe^{+2} and Mn^{+2} concentrations tend to be enriched in the dolomite of the Um Mahara Formation, varying from 1947 ppm to 8063 ppm.

4.2.2. Environment and origin of dolomite formation

The combination of the pervasive nature, the geometry of the dolomitized platform carbonates, the complete micritic replacement of the limestones, and the negative carbon and oxygen stable isotopes, as well as the regional restricted marine facies overlapping the dolomite platform, indicates that dolomitization took place in a zone of mixing of hypersaline, meteoric, and marine waters. Some evidence for freshwater influence, such as dissolution caves and pedogenic karstified features, is presented here.

Petrographically, the dolomite appears to have partly replaced the coralgal reefal grainstones and packstones (Figure 9A), as well as almost all the sparitic cementing material, phenomena that support the diagenetic origin. Moreover, the regional small sizes and the mosaic of dolomite crystals stand against the hydrothermal origin of the dolomites, which are characterized by a dominant coarse crystalline texture. Dolomite crystals generally tend to increase upwards, suggesting that hypersaline dolomitized fluid was probably more active. Dolomite luminescence shows a moderate bright orange color under CN, with occasional faint to dark zoning. The dolomite cements lining aragonite molds show that the dissolution

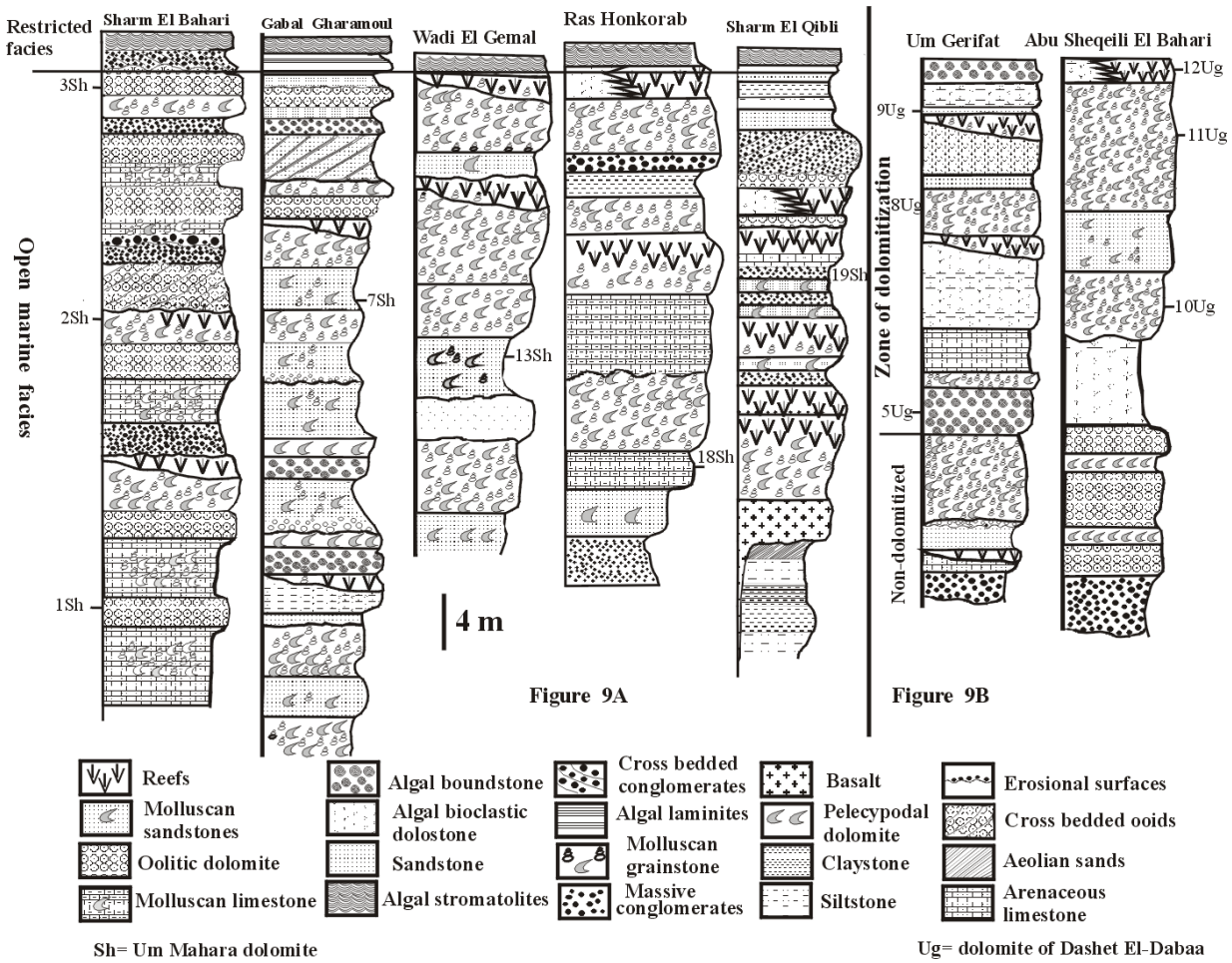

Figure 9. A) Representative measured sections of the Um Mahara Formation; for location see Figure 1. B) Representative measured sections of the Dashet El-Dabaa Member; for location, see Figure 1.

was probably preceded by complete dolomitization of the limestones, an observation that was recorded by Clegg et al. (1998) at the Abu Shaar area, west of the Gulf of Suez.

Geochemically, the Mg/Ca ratio in the dolostones of the Um Mahara Formation yielded 0.3–1.0, which indicates that the dolostones have more Ca-rich crystals, which were produced in a diagenetic mixing environment. This conclusion is in accordance with that of Randazzo and Cook (1987), who noted that Ca-rich, pervasive dolomite was precipitated in the coastal mixing zones. The relatively high concentration of Na^{+} indicates hypersaline waters, which dominated the mixing dolomitizing fluids, being consistent with the relatively higher values of Sr^{+2}. This interpretation is consistent with the interpretation of Humphrey (2000), who mentioned that dolomites rich in Sr^{+2} were formed by mixing hypersaline and marine waters.

The $\delta^{18}O$ and $\delta^{13}C$ values of the Um Mahara dolomites correspond to values reported by many authors (Gregg, 1988; Lu and Meyers, 1998; Moore et al., 1988; Swart et al., 2005) for dolomitized fluids from mixing hypersaline, fresh, and marine waters. The relative decrease in the $\delta^{13}C$ values (varying from –0.91‰ to –5.96‰) indicates that the dolomites of the Um Mahara Formation had possibly undergone geochemical alteration during diagenesis (Gregg et al., 1991). The high concentrations of Mn^{+2} and Fe^{+2} may be interpreted as being due to the large volumes of the dolomitizing meteoric water that leached the adjacent basement exposures. This high amount of Fe^{2} and Mn^{2} was also confirmed by the fact that the Um Mahara carbonate sediments in the Red Sea coastal area were a site for Fe-Mn mineralizations (Kabesh et al., 1970; Hassan, 1984). The downward depletion in Fe^{+2} values constrains fluid transport directions during dolomitization.

4.3. Dolomites of the Um Gheig Formation (late Miocene)

4.3.1. Petrography and geochemistry

The Um Gheig dolomites (up to 25 m thick) directly overlie the structurally high Abu Dabbab Evaporites. They are thinly bedded, dark gray, and hard in nature. Occasionally cryptalgal laminated and stromatolitic dolostones terminate the sequence of the Um Gheig dolomite (Gabal Gharamul and Wadi Um Gheig, see Figure 5). The beds include extensive karst features.

Petrographically, the Um Gheig dolomites are pervasive in nature. Five main types of dolostones are recognized: i- fine-grained groundmass dolomite (10–20 μm, E1 in Figure 10A); ii- coarse-zoned and iii- unzoned replacive dolomite, with an increase of planar-crystal boundaries (200 μm, E2 and E3 in Figures 10A and 10B) occurring as floating crystals, followed by alternating dolomicrite and dolosparite filling voids and microcaves (E4 in Figures 10C and 10D)**;** iv- polyhedral, spheroidal ferron; and v- saddle dolomites (300 μm, E5 in Figures 10E and 10F). Cathodoluminescence petrography has revealed that the fine-grained dolomite is dark brown-nonluminescent, replaced by yellow unzoned, luminescent dolomite. The cement and void-filling type exhibits a banded texture. The inner zone is bright yellow-luminescent, followed by a zone of dull dolomites. The outer zone is composed of alternating dull and orange-luminescent dolomite. The final phase of cementation is yellow to dull-luminescent blocky calcite (Figure 11A).

The geochemical investigation of these dolomites has proved that the MgO and CaO contents range from 18.11% to 21.938% and 32.73% to 29.91%, respectively (Table 1). The X-ray diffraction indicates that the samples are composed of either pure dolomite or dolomite with subordinated calcite and anhydrite minerals (Figure 8). Their Sr^{+2} contents range from 495 ppm to 153 ppm. The Na^{+} concentration ranges from 356 ppm to 700 ppm. The average $\delta^{18}O$ values of the fine and coarse crystalline dolomites (E2 and E3) vary from –3.94‰ PDB to –5.87‰ PDB, whereas the $\delta^{13}C$ ranges from –6.91‰ to –9.84‰ PDB. Void-filling dolomite cement has average $\delta^{18}O$ values of –7.81‰ PDB and $\delta^{13}C$ values reaching up to –10.07‰ PDB. The Fe^{+2} and Mn^{+2} concentrations tend to be relatively higher in the dolomites of the Um Gheig Formation, especially in the replacive and cement dolomites, varying from 800 ppm to 20,281 ppm. The K^{+} content varies from 41 ppm to 270 ppm (Table 1).

4.3.2. Environment and origin of dolomite formation

The early dolomite (E1) shows dull luminescent features. This, in addition to the dwarfed shells and evaporite lenses in time equivalent sediments of the Samh Member (Philobbos et al., 1989), indicates that the early dolomite was syndepositional in origin. The presence of peritidal algal laminated and stromatolitic dolomicrite that onlapped the sequence supports the syndepositional origin (Figure 11B). The fine crystalline fabric of this dolomite documents the syndepositional penecontemporaneous origin (Shukla, 1988).

The coarse crystalline dolomites (E2 and E3) that replaced the dolomicrites were probably formed by mixing reflux-evaporative brines with meteoric water. This was demarcated by $\delta^{18}O$ isotopic values that range from –3.94% to –5.87%, similar to the $\delta^{18}O$ values of evaporative reflux-meteoric water mixing dolomitization in the Smackover Formation of eastern Texas described by Moore et al. (1988). The partial replacement of their cores by calcite as interrhombic cements is related to the early influx of meteoric waters (Figure 11C) and records a mixed diagenetic setting. A similar feature was observed in the Cretaceous Eocene dolomites in northern Egypt by Holail (1991). The upwards more negative $\delta^{13}C$ values may indicate reducing conditions, being consistent with the abundance of algal laminated facies and the

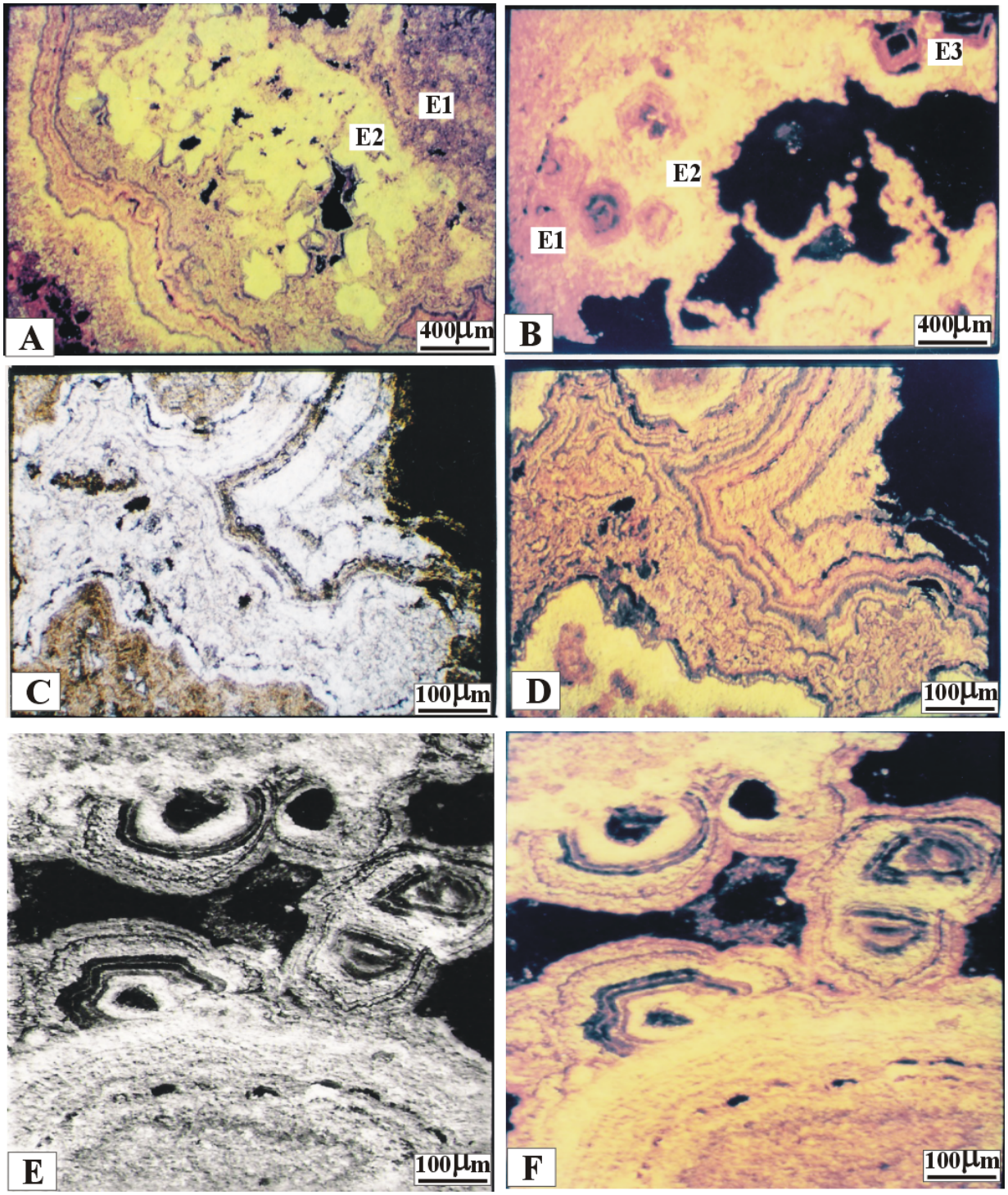

Figure 10. A) Cathodoluminescent photomicrograph of unzoned dolomite (E2) replacing the initial dolomicrite (E1); B) photomicrograph under cathodoluminescence (CL) displaying early dull luminescent (E1) replaced by bright yellow luminescent sparry dolomite and zoned dolomite (E3) characterized by alternating dull and bright luminescent zones surrounding nonluminescent iron-rich core; C) photomicrograph under polarized light displaying void-filling alternating dolomite; D) photomicrograph under cathodoluminescence (CL) displaying alternations of dull to brown luminescent bands of micritic dolomite separated by bright and orange bands of dolomicrosparite, hydrothermal cement; E) photomicrograph in plane-polarized light showing spheroidal saddle dolomite overgrowing banded dolomites in void; F) photomicrograph under cathodoluminescence (CL) showing bands of bright luminescence dolomicrite cement overgrown by saddle dolomite characterized by alternation of dull, orange, and brown luminescence zonation.

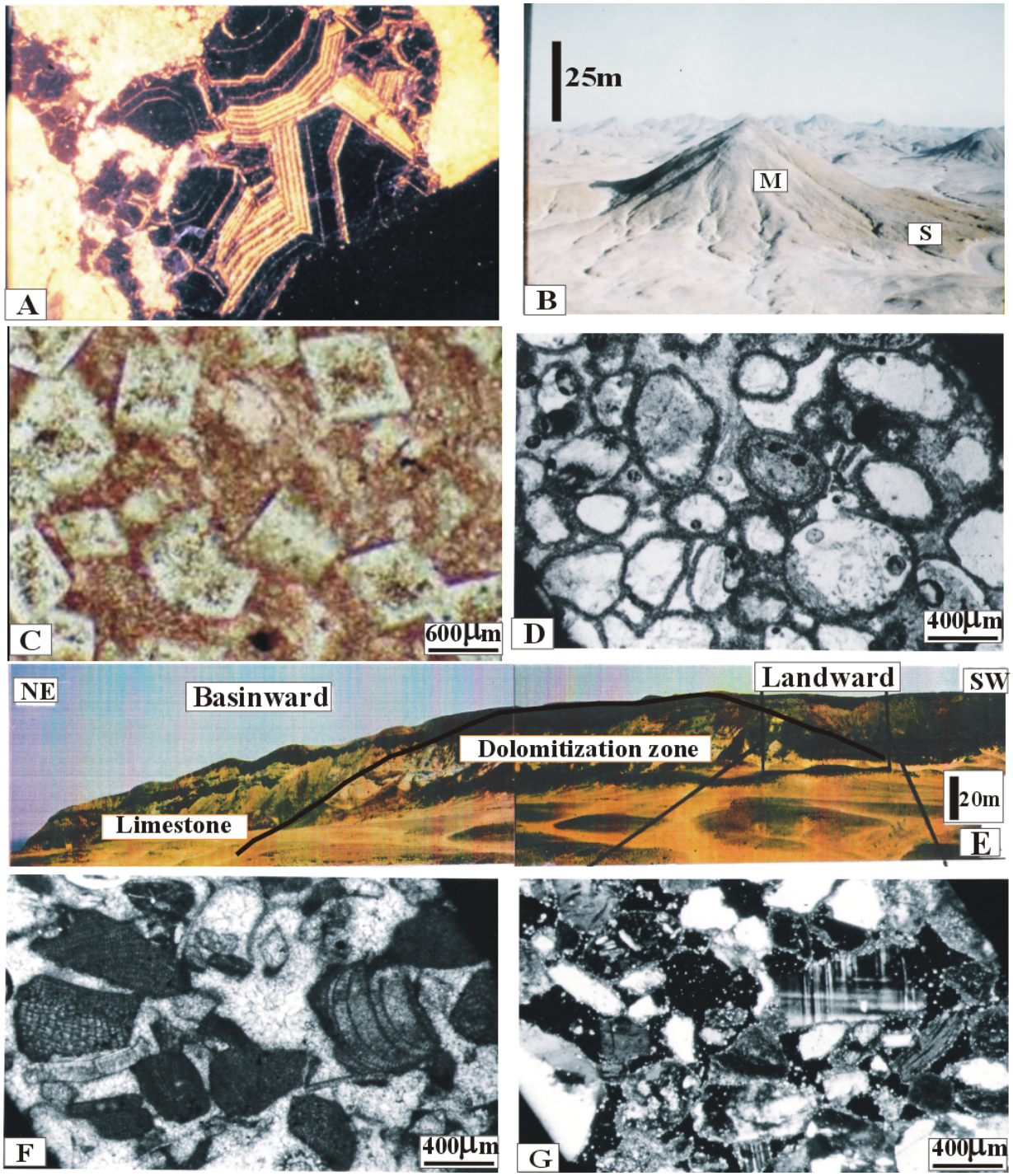

Figure 11. A) Cathodoluminescent photomicrograph displaying yellow to nonluminescent bands of void-filling calcite, Gabal Gharamoul; B) field view of Um Gheig dolomite showing stromatolites (S) downlapping massive dolomite (M), Wadi Um Gheig; C) large rhombic dolomite showing calcite replaced cloudy centers, Um Gheig dolomite; D) photomicrograph of dolomitic oolitic grainstone; E) NE-SW panorama showing the dolomitization zone of southern cliff of Dasahet El-Dabaa dome, Ras Um Gerifat; F) preservation of cellular structure of algae and other molluscan fragments despite complete replacement of cement by sparry dolomite; G) preservation of feldspars and some rock fragments within dolomitized limestones of Dashet El-Dabaa Member.

common presence of organic matter. This conclusion is in accordance with that of Longstaffe et al. (2003), who mentioned that the lower $\delta^{13}C$ values in dolomite indicate an increased contribution of carbon from organic sources.

A comparison between the Na^{+} content of dolomites E2 and E3 (356–700 ppm) with the hypersaline dolomites (1170 to 1824 ppm Na^{+}), and the mixed hypersaline-freshwater dolomites (200 to 1700 ppm Na^{+}) suggested by Gregg et al. (1991) and Lu and Meyers (1998) supports that dolomites E2 and E3 were deposited by mixing hypersaline and meteoric waters. Their Sr^{+2} concentrations are also similar to the Sr^{+2} values of mixing evaporative brines and meteoric water dolomites recorded by Lu and Meyers (1998). This supports that the Um Gheig dolomites (E2 and E3) were not produced from normal marine fluids.

The more negative values of $\delta^{18}O$ (–7.81‰) of the banded and saddle dolomite cement (E4) may be attributed to the effects of dolomitization by hydrothermal fluids. Clegg et al. (1998) mentioned that the very low $\delta^{18}O$ value is characteristic of dolostones formed under high temperatures. Ferroan spheroidal and saddle dolomites (E5) are assumed to have been formed later from hydrothermal waters that moved to higher stratigraphic levels, similar to void-filling saddle dolomite cement of the southern Irish Midlands described by Gregg et al. (2001). This is corroborated by the opinion of Warren (2000) and Davies and Smith (2007), who mentioned that dolomites of hydrothermal fluids tend to be ferroan and consist of saddle-shaped crystals, and occur as replacive and void-filling fabrics. The abundance of sulfides and iron oxide and hydroxide mineralization in the Um Gheig dolomite supports this interpretation, being consistent with the presence of high concentrations of Fe^{+2} and Mn^{+2} values (up to 20,281 ppm). The presence of vadose calcite cement indicates the influence of meteoric water during the later replacement stage of dolomite generation.

4.4. Dolomite of the Dashet El Dabaa Member of the Shagra Formation (Pliocene)

4.4.1. Petrography and Geochemistry

The Dashet El Dabaa Member lies nearer to the present Red Sea coast and interfingers westwards with the Gabir Member (Philobbos et al., 1989). It occasionally forms structural pattern involving domal and elongate anticlines limited by coastal cliffs (Purser et al., 1998). The sediments of the Dashet El Dabaa Member are composed of subtidal and intertidal sequences dominated by mixed siliciclastic, oolitic coralgal, and bioclastic carbonates (Figure 11D). Extensive dolomitization is restricted to the upper part of the central domal structures (see Figure 3A). Laterally, the dolomitized beds wedge out and change into dominantly limestones, approaching the dolomite-calcite interface (Figure 11E). The vertical distribution of the dolomite exhibits a distinct dolomitization gradient from 100% dolomite near the surface to less than 10% dolomite downward (see Figure 9B).

Petrographically, the dolomite mimetically replaced all the sparitic material occurring as a cementing material and often shows surprisingly good preservation of microstructure, particularly in molluscan and coralline algal clasts (Figure 11F). The dolomite exists as euhedral rhombs with thin clear rims ranging from 10 μm to 30 μm. Occasionally zoned dolomites with clear outer rims and cloudy centers, ranging from 50 μm to 80 μm, are encountered. The cathodoluminescence of the dolomite crystals is dull to uniformly dark brown, while zoned dolomites range from bright yellow to yellowish brown luminescence.

Geochemically, the dolomite is Ca-rich (1.49–2.88). Its Sr^{+2} content ranges between 20 ppm and 250 ppm, with an average of 177 ppm. Na^{+} content is up to 853 ppm. Four samples have high Na^{+} concentrations ranging from 2529 ppm to 6847 ppm. The dolomite of the Dashet El Dabaa Member is Fe^{+2}-rich (varying from 1692 ppm to 3049 ppm) and Mn^{+2}-poor (varying from 109 ppm and 219 ppm). Oxygen isotopes have values between 2.66‰ PDB and 3.23‰ PDB, and carbon isotopes have values between –10.86‰ PDB and -13.03‰ PDB. X-ray diffraction indicates the presence of gypsum, anhydrites, and unstable feldspars (microcline, albite, and anorthite).

4.4.2. Environment and origin of dolomite formation

The Mg/Ca ratio in the Pliocene dolostones varies between 0.3 and 1.0, indicating that they were precipitated from water of lower Mg/Ca ratios. This was interpreted, according to the opinion of Land (1991), as dolomites having been formed by mixed refluxing restricted hypersaline and marine waters. The downward diminution of dolomites is probably related to the penetration depth of those mixing waters.

Isotopically, the dolomite of the Dashet El Dabaa Member has general positive isotopic signatures documenting that hypersaline sea water has been involved for dolomitization. The fall in the ranges of the $\delta^{18}O$ values is also due to the hypersaline dolomitizing fluid, as suggested by Land (1983). The presence of gypsum and anhydrite minerals in the dolomitized carbonates supports hypersalinity. This interpretation is seemingly consistent with the excellent preservation of unstable feldspars within the dolomitized carbonates. Feldspar grains, such as albite, microcline, and anorthite (determined by X-ray diffraction), and feldspar-rich basement clasts exhibiting no corrosion (Figure 11G) within dolomites exclude the effect of meteoric weathering and indicate that no significant amounts of surface meteoric waters played a role in the dolomitization process. The absence of recrystallized dolomite is another piece of evidence that precludes the involvement of meteoric waters during dolomitization.

The highly depleted carbon isotope values of the Dashet El Dabaa dolomites (up to –13‰ $\delta^{13}C$) probably indicate the involvement of hydrocarbons that migrated from the middle Miocene evaporites outcropping at the west of the dolomitized beds. This interpretation is supported by the observation of Clegg et al. (1998) at Abu Shaar, west of the Gulf of Suez. The low Sr^{+2} concentrations are interpreted as being probably related to the higher depletion that resulted from interaction with near surface-meteoric groundwater after dolomite formation, and/or as being related to the replaced sediment comprising aragonite poor in Sr^{+2} (Veizer et al., 1978). The Na^{+} content tends to be high in some samples (up to 6847 ppm), indicating the enrichment of these samples by sodic feldspars, which were identified by X-ray diffraction. The increase of Fe^{+2} content may suggest that the clastics intercalating dolomites were the source of Fe^{+2} during dolomitization.

5. Proposed depositional models for the Neogene dolomites: effects of eustasy, tectonics, and paleoclimate

5.1. The Um Diheisi dolomitization model

During the initial rift development, half grabens limited by 100°–120° and 140° fault directions with gentle dip-slope tilted blocks were generated (Tarabili, 1966). Tilting of blocks is indicated by slope deposits composed of slumped and brecciated dolomites, which dip 30° downslope along fault scarps (El Haddad et al., 1984).

The deposition of the Um Diheisi Member started with the sea level rise. This led to accumulations of transgressive deposits composed of restricted subtidal facies, which occurred in the shallow structural depressions. Dolomitization would be limited in these sediments because the accommodation space rapidly increased in the depressions, but laterally towards the structural highs (fault scarps and crests of blocks areas), which acted as sites of lowstand restricted peritidal settings with reduced accommodation space, dolomitization developed penecontemporaneous with shallowing-upward peritidal deposition (Figure 12A).

By the end of the Um Diheisi deposition, during the continued short-term sea level falling and/or due to the repeated tilting of blocks, transgressive and lowstand progradational meter-scale peritidal cycles dominated. The dolomitization began during the regressive stage of high-frequency sea level cycles when tidal flats prograded onto the lagoonal deposits due to a sea level fall, and prior to the beginning of deposition of the next cycle (Figure 12B). In this case the dolomitization was formed by downward percolating and seaward flow of evaporated seawater (Figure 12C). This is supported by the common occurrence of dolomitized rip-up clasts at the base of the upper cycle.

The continued falling of sea level and the increase of restriction due to isolation of grabens by intervening structural uplift allowed the sudden lateral shift in paleoenvironments and facies from dolomites to dominant evaporites (Roza Evaporites, Figure 12D).

Climatically, the intense and pervasive dolomitization nature, with periodic subaerial exposure, and the relatively heaviest $\delta^{18}O$ values of the Um Diheisi Member reflect an arid climate, which prevailed through initial dolomitization. This interpretation is consistent with that of Haas and Demeny (2002), who mentioned that in arid conditions the intense evaporation causes pervasive dolomitization with a positive shift in the oxygen isotope composition. Kuznetsov (1991) mentioned that in arid climates the primary deposition of magnesium in tidal and sabkha facies is considerable. The aridity that prevailed at that time is further evidenced by the abundance of aeolian sands, unstable feldspar grains, and flash flood-debris flow conglomerates including feldspar-rich basement clasts of the time equivalent to the deposition of the Um Abas Member (Philobbos et al., 1989). Occasionally, the dominantly arid climate was interrupted by humid seasons, marked by the presence of some recrystallized zoned dolomite at the top of each cycle and the abundance of soil horizons' intercalations and fine terrigenous materials near the disconformable surfaces.

5.2. The Um Mahara dolomitization model

Based on the field studies and sequence stratigraphic distribution, two dolomitization phases could be detected in the Um Mahara Formation. The earlier dolomitization phase (Figure 13A) occurred in the carbonate platform tilted westwards towards the rift periphery (e.g., at Sharm El Qibli, Abu Shegeili El Bahari, south of Um Gheig, Gabal Gharamoul), and within structural depressions forming marine bays at the southern ends of the basement blocks (e.g., Ras Honkorab). In this case, the marine fluids were probably pushed by surface currents' up-dip towards the crest of the low-lying block and then penetrated into a permeable, inclined sedimentary talus. Due to the inclination of the beds westwards, the hydrodynamic flow involving the passage of large volumes of the interstitial marine waters, which intermixed with saline waters, was developed due to the isolation of sea water within those depressions. The resultant mixing of dolomitizing fluids migrated downwards throughout the substrata, causing dolomitization. Purser et al. (1987) described Quaternary grabens having different sedimentary composition near Hamata (24°16′N, and 35°26′E); the western grabens include dolomites and sulfates, whereas the eastern ones include siliciclastics and limestones.

The late dolomitization phase was regional and took place by the end of the deposition of the main eastward prograding open marine coralgal bioclastic limestone

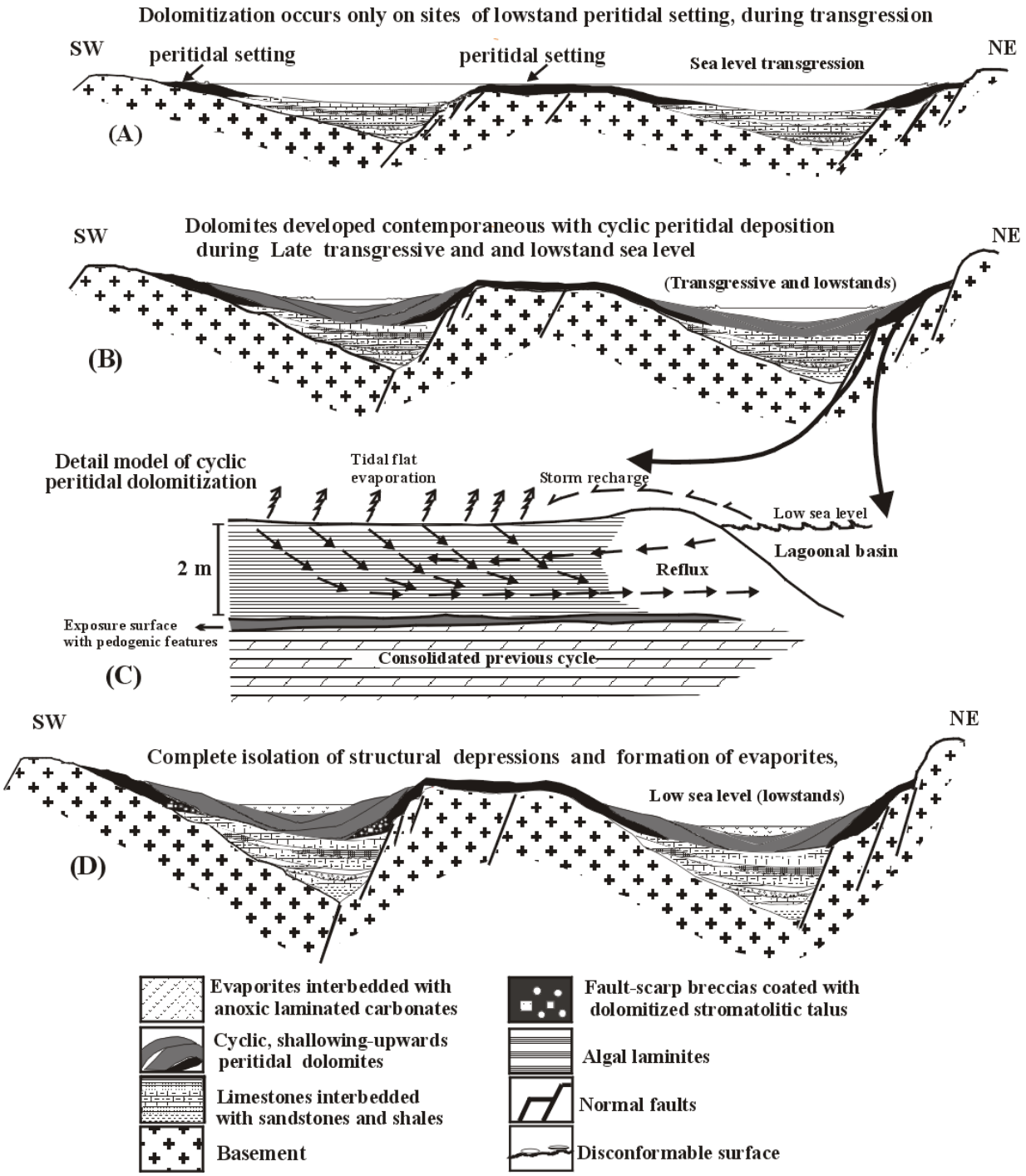

Figure 12. Stages of Um Deheisi sedimentation (A, B, D) and conceptual model for dolomitization (C).

platform (Figure 13B). This was followed by a renewed uplift of the west shoulders, leading to exposure of the platform and vertical infiltration of meteoric waters (Figure 13C), which caused the dissolution of limestones of the platform and formation of meteoric diagenetic fabrics as moldic and vuggy porosity and cavities. The occurrence of karst surface with pedogenic features like calcrete layers and the coarse fanglomerates overlying directly the platform dolomites document the action of meteoric water, indicating that prevailing humid conditions were preceded by dolomitization process. Purser (1998) noticed large dissolution cavities within the mid-Miocene open

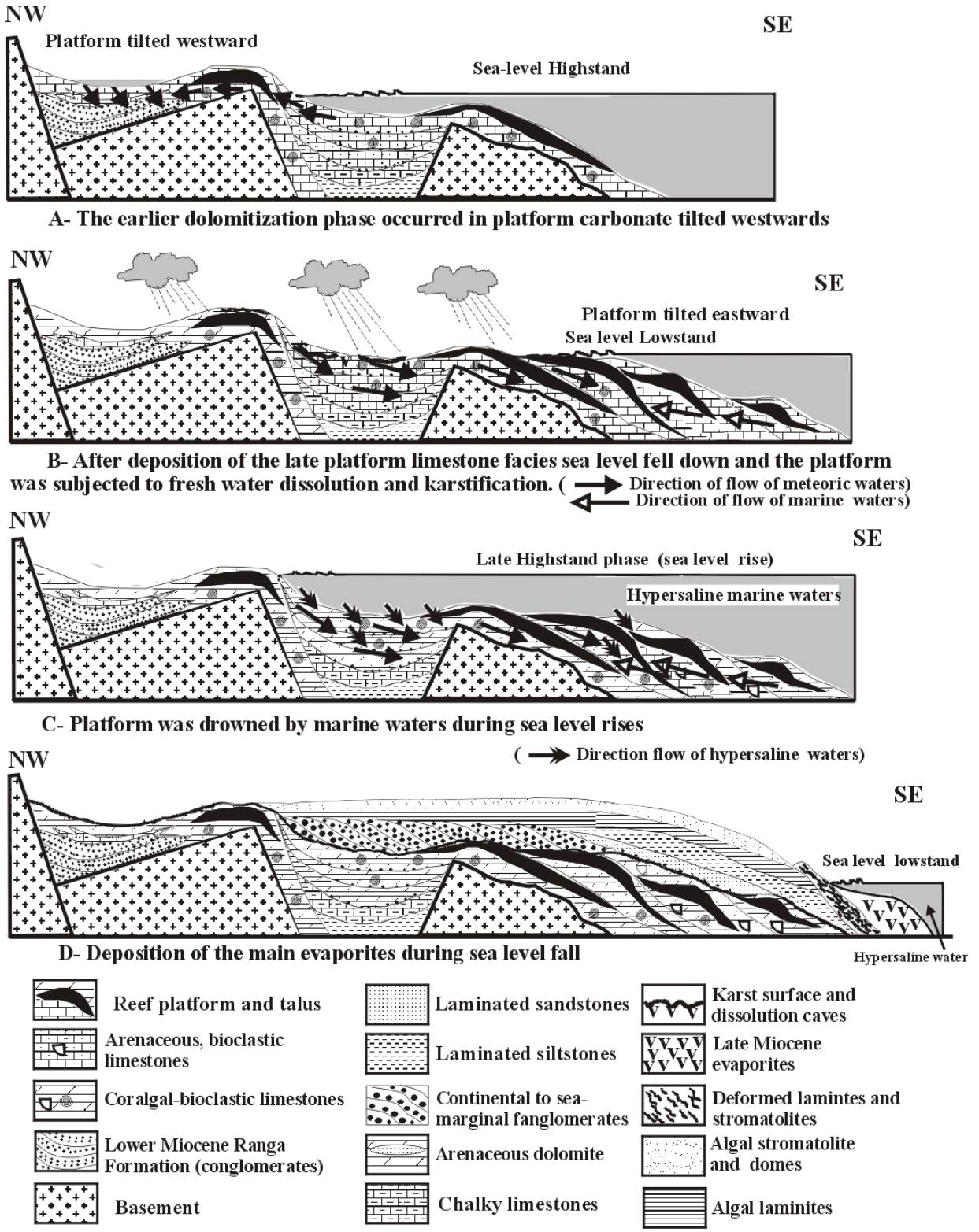

Figure 13. Proposed model for dolomitization of the platform facies of the Um Mahara Formation by mixing waters.

marine platform. Later on, the limestone platform was drowned by hypersaline marine waters, in which restricted algally laminated and stromatolitic carbonate facies were formed. The latter facies extends along the northwest Red Sea and the Gulf of Suez, covering the platform facies. Purser et al. (1998) stated that those hypersaline conditions record a rise of relative sea level prior to the onset of the main Miocene Abu Dabbab evaporite sedimentation. The hypersaline fluids were infiltrated downward by density contrast into the open marine platform facies, mixing with two pore waters: meteoric and marine waters. As relative sea level continued to fall and the general eastward inclination of the beds stayed fixed, the interstitially mixed three waters migrated downward and seaward through the prograded carbonate platform, causing dolomitization of the sequence (Figures 13C and 13D).

Following the dolomite formation and uplifting of the whole middle Miocene platform and lowering of sea level, the area was subjected to meteoric waters again. This led to the progressive freshening of the mixing zone, which caused leaching of dolomite crystal cores and corrosion of crystal faces. The presence of the karst surface including calcrete layers and soil horizons, as well as the vadose calcite cement on top of the platform, display meteoric water influences.

5.3. The Um Gheig dolomitization model

Based on the favorable geologic setting, geochemistry, and petrographic characteristics, three events for the dolomitization history of the sediments of the Um Gheig Formation are considered (Figure 14):

1) The early dolomite (E1) that constitutes the bulk of the Um Gheig dolomite overlies the main Abu Dabbab evaporates and involved horizontal flow of hypersaline brines during early restriction conditions. It is believed that this restricted setting was probably associated with the global sea level fall in late Messinian times and prior to complete opening during the Pliocene, as revealed by Orszag-Sperber et al. (1998). Extensive evaporite deposition in stratigraphically equivalent basinal sediments of the Samh Member points toward pronounced lowstand basin restriction.

2) By the end of the initial dolomite formation (E1), and during humid climate and lower sea level, a mixture of refluxing hypersaline and meteoric waters took place, leading to formation of replacive zoned and unzoned dolomites (E2 and E3).

3) The global fall of sea level associated with the second phase of the Red Sea rifting and the prevailing humid conditions led to the formation of large dissolution caves, fractures, and microkarsts (Figure 14). These humid diagenetic features were supported by the occurrence of time equivalent fluvial clastic sediments of the Samh Member (Philobbos et al., 1989). Following this stage, the Um Gheig dolomites were exposed to hydrothermal fluids rising through faults, which acted as conduits for these fluids into voids and fractures. Initially, these hydrothermal fluids caused the precipitation of alternating banded dolomites (E4). The last stage of hydrothermal dolomitization (void-filling cement) was dominated by deposition of nonplanar, spheroidal ferroan and saddle dolomites (E5). Occasionally the heated fluids led to a neomorphic recrystallization of the dolomicrite (E1) to a coarser zoned crystalline planar dolomite. A similar feature was observed in Jurassic dolostone in Lebanon, as described by Nader et al. (2004). The final filling of these voids and caves was dominated by a vadose calcite (Figure 15).

5.4. The Dashet El Dabaa dolomitization model

Syn-Pliocene tectonics in the form of rejuvenation of clysmic (N40°W) and cross faults (NE) and evaporite remobilization were the main factors controlling dolomitization of the Dashet El Dabaa Member of the Shagra Formation as follows: during the deposition of the upper part of the Dashet El Dabaa Member, NW synsedimentary faulting in combination with the underlying diapirism took place, leading to the formation of NW paleohighs (domal and elongate anticlines, at Ras Um Gerifat, Abu Shegeili El Bahari, and Ras Samadai) parallel to the shoreline. The structural paleohighs can be explained by the lateral thickening and marked lateral facies changes, indicating that these faults were active during Pliocene times (Mahran, 2000). The progressive uplift of the paleohighs stimulated the establishment of sheltered areas to west of them (Figure 16). Waters situated within those areas, separated from the open sea by barriers, logically would evolve towards hypersalinity. Resulting differences in density caused the percolation of the interstitial waters through barriers, and mixing with sea waters evolving dolomitization. This dolomitization took place probably at the end of the late highstand and might be extensive during sea level fall and lowstands. The seaward progradation of the shoreline and the tilted nature of the sediment/water interface had possibly been accompanied by a migration of the hypersaline dolomitized zone seaward. This is evidenced by the geometry of the dolomite body, thick in the east but thinning westwards in the landward direction.

6. Conclusions

1) Most of the Neogene carbonate platforms in the Red Sea area have been partially to pervasively dolomitized. The intensity of the dolomitization depends on the chemical composition of the interstitial dolomitizing waters and on their lateral and vertical movements as well as the inclined nature of the sediment/water interfaces.

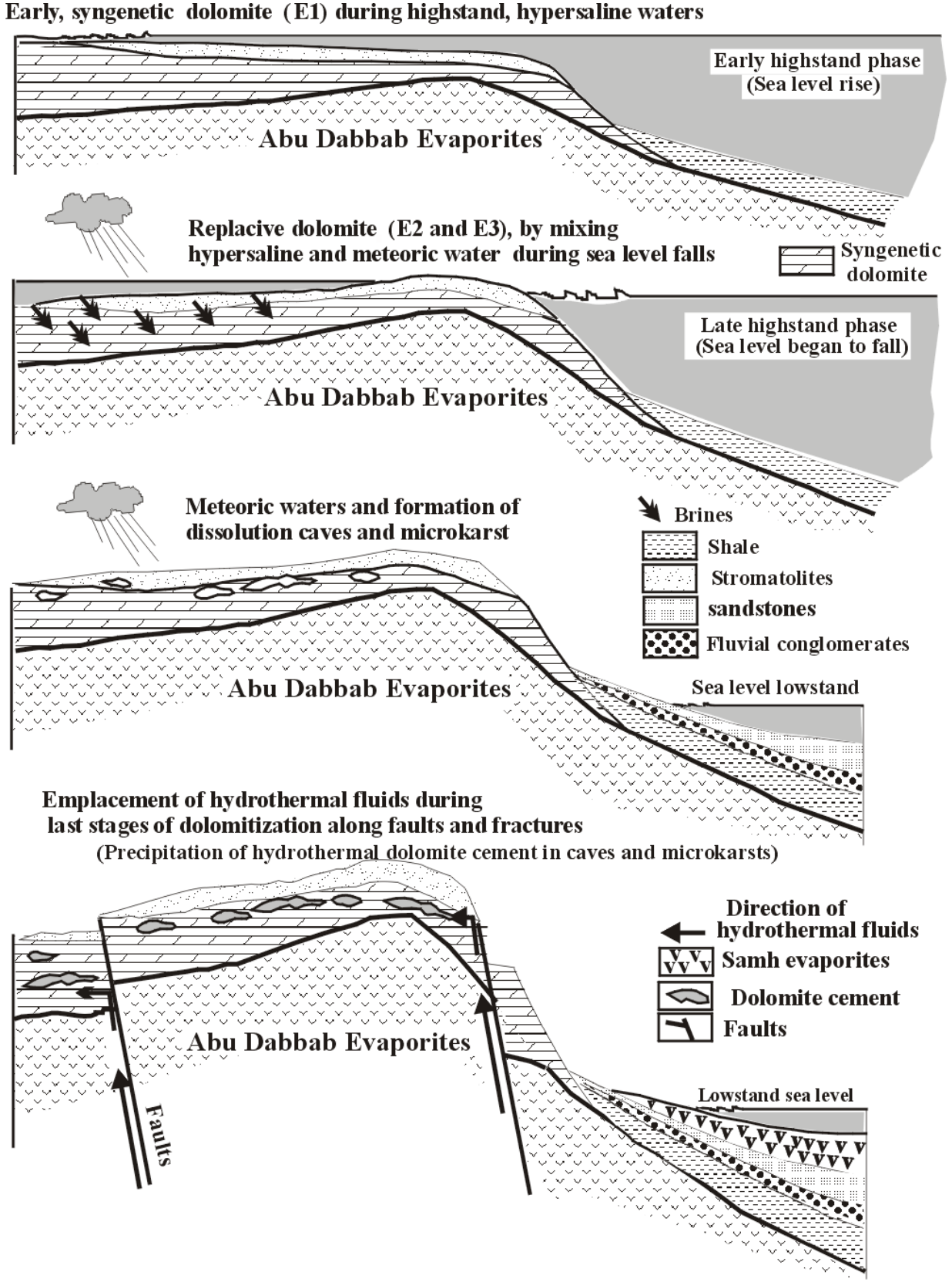

Figure 14. Proposed stages for the dolomitization of the sediments of the Um Gheig Formation.

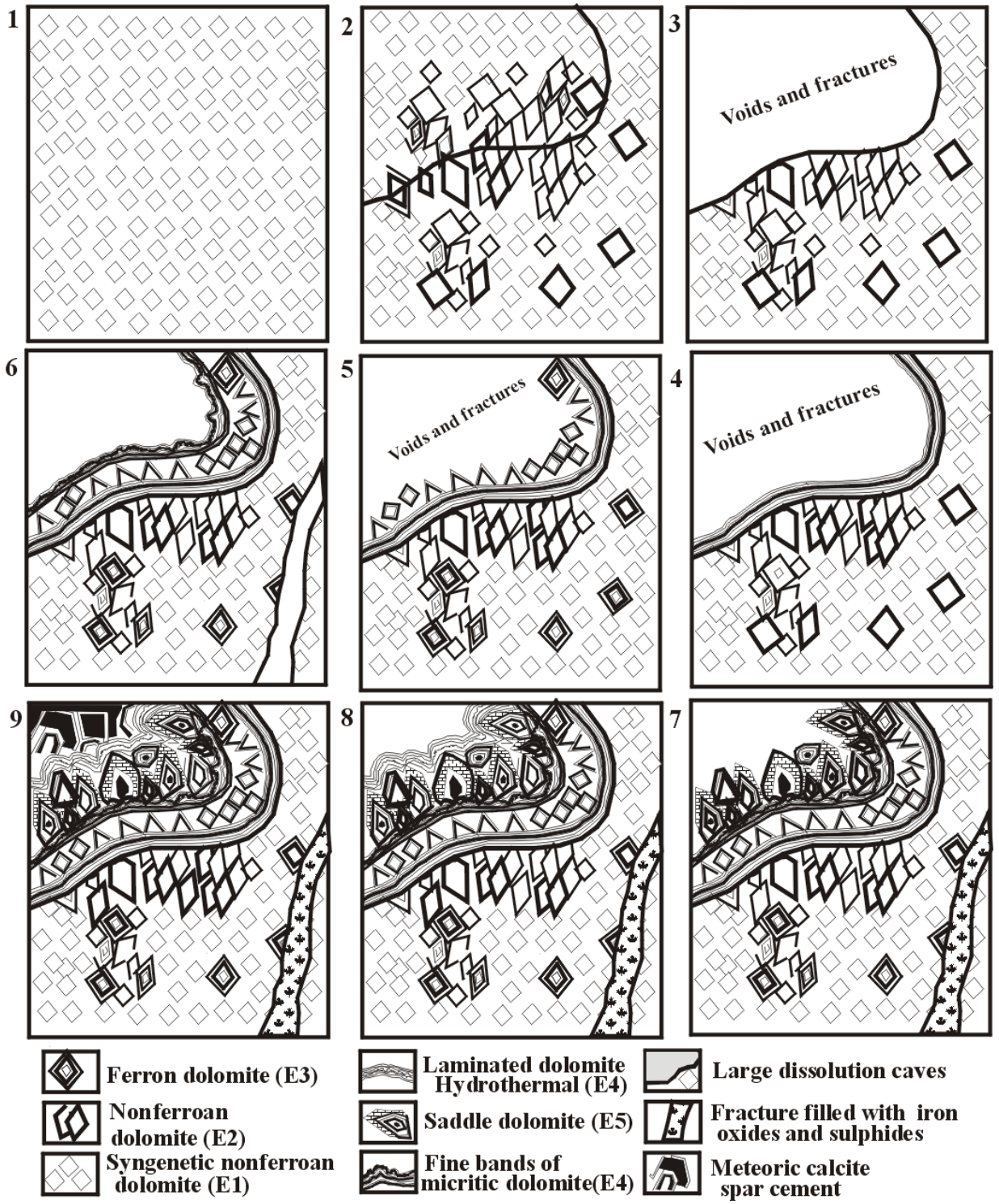

Figure 15. Schematic diagram summarizing various episodes of dolomite formation in the Um Gheig Formation.

2) Petrographic study, cathodoluminescence supported by geochemical data (major elements, trace elements, and stable isotopes), and geological setting have provided the basis for interpreting the Neogene dolomites. i- The early Miocene Um Diheisi finely laminated dolomicrites formed syndepositionally from hypersaline marine waters in a restricted peritidal environment; ii- the middle Miocene Um Mahara dolomite resulted from a

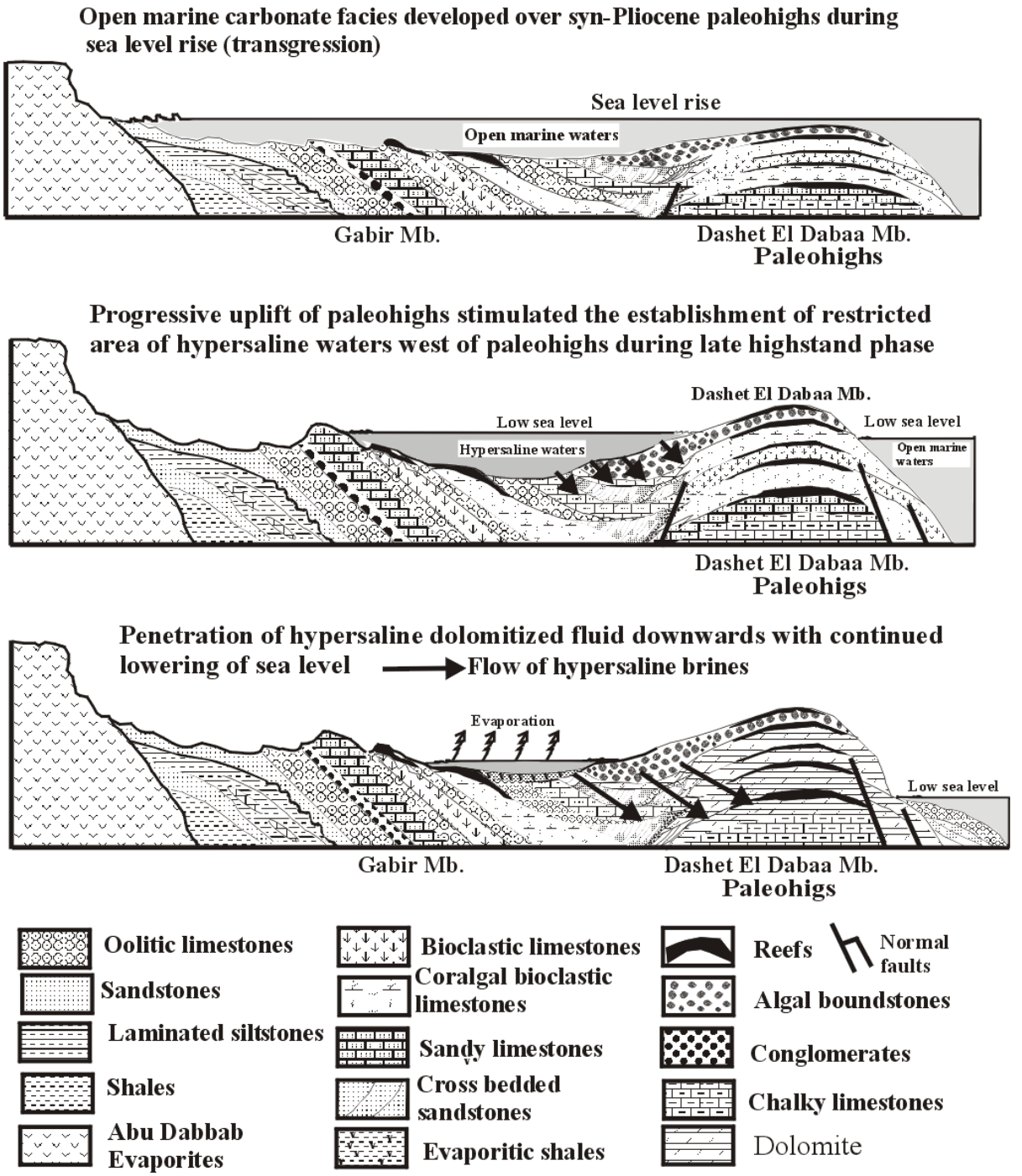

Figure 16. Model for dolomitization of the Dashet El-Dabaa Member.

regional replacement, which originated through mixing of three waters: meteoric, marine, and hypersaline; iii- late Miocene Um Gheig dolomites that occur as mixed penecontemporaneous, replacive, and cement types are proposed to have developed by multiple dolomitization events by fluids varying from evaporative brines to mixing reflux evaporative and meteoric waters and later hydrothermal; iv- Pliocene Dashet El Dabaa replacive dolomite formed by mixtures of marine and hypersaline waters.

3) Geochemically, the relative depletion in $\delta^{18}O$ values in the diagenetic dolomites of the Um Mahara and late dolomitization phases of the Um Gheig may have resulted from the meteoric water and hydrothermal components in the fluid that produced dolomites. On the contrary, the relatively heaviest $\delta^{18}O$ values in the dolomites of the Um Diheisi, the syndepositional type of the Um Gheig, and the Dashet El Dabaa Member support a hypersaline source for the dolomitizing fluid. This is consistent with the enrichment in Na^{+} content compared to the diagenetic dolomites. These differences are also reflected in the dolomite fabric; penecontemporaneous dolomites are more finely crystalline than diagenetic dolomites. The CaO contents of the Um Gheig and Dashet El Dabaa dolomites are higher relative to other dolomites. Dashet El Dabaa dolomite contains less Fe^{+2} and Mn^{+2} relative to the other dolomites. It is believed that the resulting chemical compositions indicate that the Neogene dolomites may have undergone significant geochemical alteration during diagenesis in the depositional environments.

4) The syn-rift irregular morphotectonic relief and eustasy have strongly influenced the dolomitization processes of the Neogene carbonates. The Um Diheisi dolomitization occurred with cyclic peritidal deposition in local half graben basins, related to sea transgression interrupted by short-term sea level falls. The dolomitization history of the Um Mahara Formation is believed to have occurred in two stages. The first is limited to the westward-tilted platform and isolated depressions when hypersaline waters were developed, and later intermixed with refluxing marine waters. The second stage of dolomitization took place after deposition of the main eastward prograding limestone platform, initially when the platform was exposed to meteoric and marine waters and subsequently drowned by hypersaline brines. As a result of progressive fall in sea level, the mixed dolomitizing fluids migrated downward and eastward through the platform sediments, forming regional dolomitization. In the Um Gheig dolomites, there were three episodes of dolomitization, i- penecontemporaneous dolomitization associated with early restricted phases, ii- mixing of refluxed evaporative and meteoric waters that caused dolomitization associated with late highstands and lowstands, and iii- the latest dolomitization phase occurring as dolomite cement formed by hydrothermal fluids during the exposure periods of the Um Gheig Formation. Dolomitization of the Pliocene Dashet El Dabaa Member involved mixtures of hypersaline and marine waters that had possibly occurred initially during the late highstands, but probably became extensive during lowstands and the falling of sea level associated with syn-Pliocene tectonics.

5) Paleoclimate is probably the main factor invoked to explain the possible dolomitization models. An arid climate prevailed during the Um Diheisi dolomicrite and the early dolomitization phase of Um Gheig, in which evaporative, hypersaline brines would have likely developed in a restricted peritidal and reflux-type lagoonal setting. With predominate humidity and periodic freshwater invasion (as in the case of the replacive, pervasive dolomites of the Um Mahara and late dolomitization phase of the Um Gheig dolomites), the meteoric water migrated seawards and downwards. Along with the possible porosity enhancement, as a result of dissolution and leaching of precursor carbonates, dolomitization took place within the zone of mixing waters. The arid conditions returned during Pliocene deposition, evolving the waters in the sheltered areas towards hypersalinity.

Acknowledgment

The author is greatly indebted to Prof Dr Tawfiq Mahran, Geology Department, Faculty of Science, Sohag University, for his assistance during a field trip and for reading the manuscript.

References

Aissaoui D, Coniglio M, James P, Purser B (1986). Diagenesis of a Miocene reef platform: Jabal Abu Shaar, Gulf of Suez, Egypt. In: Schreoder J, Purser B, editors. Reef Diagenesis. Berlin, Germany: Springer-Verlag, pp. 112-131.

Akkad A, Dardir AA (1966). Geology of the Red Sea Coast between Ras Shagra and Marsa Alam, Egypt. Cairo, Egypt: Geological Survey of Egypt, Paper No. 35.

Balog A, Read F, Hass J (1999). Climate-controlled early dolomite, Late Triassic platform carbonates, Hungary. J Sediment Research 69: 267-282.

Baum G, Harris W, Drez P, (1985). Origin of dolomite in the Castle Hayne limestone, North Carolina. J Sediment Petrol 55: 507-517.

Bosence D, Wood J, Rose E, Qing H (2000). Low- and high-frequency sea level changes control peritidal carbonate cycles, facies and dolomitization in the Rock of Gilbraltar (Early Jurassic, Iberian Peninsula). J Geol Soc London 157: 71-74.

Clegg N, Harwood G, Kendall A (1998). The dolomitization and post-dolomite diagenesis of Miocene platform carbonates: Abu Shaar, Gulf of Suez, Egypt. In: Purser BH, Bosence DWJ, editors. Sedimentation and Tectonics of Rift Basins: Red Sea - Gulf of Aden. London, UK: Chapman and Hall, pp. 390-405.

Coniglio M, James NP, Aissoui DN (1988). Dolomitization of Miocene carbonates, Gulf of Suez, Egypt. J Sediment Petrol 58: 100-119.

Davies GR, Smith LB (2007). Structurally controlled hydrothermal dolomite reservoir facies: an overview. AAPG Bull 90: 1741-1790.

Dickson JA (1966). Carbonate identification and genesis as revealed by staining. J Sediment Petrol 37: 491-505.

El-Haddad A (2004). Evaporative sea level draw down: a new model for the regional dolomitization of the Miocene carbonates of the Red Sea and Gulf of Suez, Egypt. Annals Geological Surv Egypt 26: 245-271.

El-Haddad AA, Aissaoui D, Soliman M (1984). Mixed carbonate-siliciclastic sedimentation on a Miocene fault- block, Gulf of Suez, Egypt. Sediment Geol 37: 185-202.

El-Shater AA, Philobbos ER (1998). Clay minerals association of the syn-rift sediments of the southern Egyptian red Sea coastal areas: a tectonic sedimentary approach, Egypt. Egyptian Journal of Geology 44: 597-720.

Gorody W (1980). The Lower Ordovician Mascot Formation, Upper Knot Group, in north-central Tennessee. PhD, Rice University, Houston, Texas.

Gregg JM (1988). Origins of dolomite in the offshore facies of the Bonneterre Formation (Cambrian), Southeast Missouri. In: Shukla V, Baker PA, editors. Sedimentology and Geochemistry of Dolostones. Tulsa, OK, USA: SEPM Special Publications, pp. 77-93.

Gregg JM, Howard SA, Mazzullo SJ (1991). Early diagenetic recrystallization of recent, peritidal dolomites, Ambergris Cay, Belize. In: Bosellini A, Brandner R, Flugel E, Purser B, Schlager W, Tucker M, Zenger D, editors. Dolomieu Conference on Carbonate Platforms and Dolomitization (Abstracts), Italy, 12–17 September 1991, p. 97.

Gregg J, Shelton K, Johnson A, Somerville I, Wright W (2001). Dolomitization of the Waulsortian limestone (Lower Carboniferous) in the Irish Midlands. Sedimentology 48: 745-766.

Haas JM, Demeny A (2002). Early dolomitization of Late Triassic platform carbonates in the Transdanubian Range, Hungary. Sediment Geol 151: 225-242.

Hassan MM (1984). Contribution to the studies of Pb-Zn and Fe-Mn mineralization in the Red Sea coastal zone (abstract). In: 1st Symposium of Phanerozoic and Development, Egypt.

Holail H (1991). Geochemical signatures in the Upper Cretaceous-Middle Eocene dolomites and their relation to deposition and diagenesis, Northern Egypt. In: Bosellini A, Brandner B, Flugel E, Purser B, Schlager W, Tucker M, Zenger D, editors. Dolomieu Conference on Carbonate Platforms and Dolomitization (Abstracts), Italy, 12–17 September 1991, p. 111.

Humphrey JD (2000). New geochemical support for mixing zone dolomitization at Golden Grove, Barbados. J Sediment Res 70: 1160-1170.

Iannace A, Frisia S (1991). Changes in dolomitization patterns between Norian and Rhaetian in the Southern Tethys realm: clues to the dolomitization of the Dolomia Principle. In: Bosellini A, Brandner B, Flugel E, Purser B, Schlager W, Tucker M, Zenger D, editors. Dolomieu Conference on Carbonate Platforms and Dolomitization (Abstracts), Italy, 12–17 September 1991, p. 120.

Issawi B, Francis M, El Hinnawi M, Mahanna A, El Deftar I (1971). Geology of Safaga- Quseir coastal plain and of Mohamed Rabah area. Annals of the Geological Survey of Egypt 1: 1-20.

Jadoul F, Berra F, Frisia S (1991). Tectonics and sea level changes as controlling factors in the evolution of an inner carbonate platform and related intra-platform basins: an example from the Norian of Lombardy, Southern Alps. In: Bosellini A, Brandner B, Flugel E, Purser B, Schlager W, Tucker M, Zenger D, editors. Dolomieu Conference on Carbonate Platforms and Dolomitization (Abstracts), Italy, 12–17 September 1991, pp. 123-124.

Kabesh ML, El-Hinnawi E, Mansour, MA (1970). A note on the geochemistry of the iron ochre deposits of Um Gerifat, Red Sea, Egypt. UAR Journal of Geology 14: 43-46.

Khalifa MA, Abu El Hassan MA (1993). Lithofacies, cyclicity, diagenesis and depositional environments of the Upper Cenomanian, El-Heiz Formation, Bahariya Oasis, Western Desert, Egypt. J Afr Earth Sci 17: 555-570.

Kuznetsov VG (1991). Dolomite in carbonate formations in various climatic zones. In: Bosellini A, Brandner B, Flugel E, Purser B, Schlager W, Tucker M, Zenger D, editors. Dolomieu Conference on Carbonate Platforms and Dolomitization (Abstracts), Italy, 12–17 September 1991, p. 142.

Land LS (1983). The application of stable isotopes to studies of the origin of dolomite and to problems of diagenesis of clastic sediments. In: Arthur MA, Anderson TF, Kaplan IR, Veizer J, Land LS, editors. Stable Isotopes in Sedimentary Geology. Short Course 10. Tulsa, OK, USA: SEPM, pp. 1-22.

Land LS (1991). Dolomitization models: sea water and mixing zones. In: Bosellini A, Brandner B, Flugel E, Purser B, Schlager W, Tucker M, Zenger D, editors. Dolomieu Conference on Carbonate Platforms and Dolomitization (Abstracts), Italy, 12–17 September 1991, p. 144.

Land LS, Hoops GK (1973). Sodium in carbonate sediments and rocks; A possible index to the salinity of diagenetic solutions. J Sediment Petrol 43: 714-717.

Longstaffe F, Calvo R, Ayalon A, Donaldson S, (2003). Stable isotope for multiple fluid regimes during carbonate cementation of the Upper Tertiary Hazeva Formation, Dead Sea Graben, southern Israel. J Geochem Explor 80: 151-170.

Lu FH, Meyers WJ (1998). Massive dolomitization of a late Miocene carbonate platform: a case of mixed evaporative brines with meteoric water, Nijar, Spain. Sedimentology 45: 263-277.

Mahran T, El Shater A, Sadeik S (2007). Sedimentology and sequence stratigraphy of Oligocene-Middle Miocene sediments in the area south of Wadi Um Gheig, Red Sea, Egypt**:** effects of eustasy and tectonics. In: The 45th Annual Meeting of the Geological Society of Egypt (Abstracts).

Mahran TM (2000). Cyclicity and sequence stratigraphy of syn-rift Late Neogene mixed carbonates- siliciclastics of the area between Wadi Zug El Bohar and Wadi Dabr, Red Sea, Egypt. Egyptian Journal of Geology 44: 237-275.

Montanez P, Read F (1992). Eustatic control on early dolomitization of cyclic peritidal carbonates: evidence from the Early Ordovician Upper Knox Group, Appalachians. Geol Soc Am Bull 104: 872-887.

Montenant C, Ott d'Estevou P, Jarrege J, Richert JP (1998). Rift development in the Gulf of Suez and NW Red Sea: structural aspects and related sedimentary processes. In: Purser BH, Bosence DWG, editors. Sedimentation and Tectonics of Rift Basins: Red Sea - Gulf of Aden. London, UK: Chapman and Hall, pp. 97-117.

Montenant C, Ott d'Estevou P, Purser BH, Burollet PT, Jarrige JJ, Orszag-Sperber F, Philobbos E, Plaziat JC, Part P, Richert JP et al. (1988). Tectonic and sedimentary evolution of the Gulf of Suez and the northwestern Red Sea. Tectonophysics 153: 161-177.

Moore CH (1989). Carbonate Diagenesis and Porosity. Developments in Sedimentology. Amsterdam, the Netherlands: Elsevier.

Moore CH, Chowdhury A, Chan L (1988). Upper Jurassic smackover platform dolomitization, northwestern Gulf of Mexico: a tale of two waters. In: Shukla V, Baker PA, editors. Sedimentology and Geochemistry of Dolostones. Tulsa, OK, USA: SEPM Special Publications, pp. 175-190.

Mresah MH (1998). The massive dolomitization of platformal and basinal sequences: proposed models from the Paleocene, Northeast Sirte Basin, Libya. Sediment Geol 116: 199-226.

Nader F, Swennen R, Ellam R (2004). Reflux stratabound dolostone and hydrothermal volcanism-associated dolostone: a two-stage dolomitization model (Jurassic, Lebanon). Sedimentology 51: 339-360.

Nedelec A, Affaton P, France-Lanord C, Charriere A, Alvaro J (2007). Sedimentology and chemostratigraphy of the Bwipe Neoproterozoic cap dolostones (Ghana, Volta Basin): a record of microbial activity in a peritidal environment. C R Geosci 339: 223-239.

Nicolaides S (1995). Origin and modification of Cambrian dolomites (Red Heart dolomite and Arthur Creek Formation), Georgina Basin, Central Australia. Sedimentology 42: 249-266.

Orszag-Sperber F, Purser B, Rioual M, Plaziat J (1998). Post-Miocene sedimentation and rift dynamics in the southern Gulf of Suez and northern Red Sea. In: Purser BH, Bosence DWG, editors. Sedimentation and Tectonics of Rift Basins: Red Sea - Gulf of Aden. London, UK: Chapman and Hall, pp. 427-447.

Philobbos ER, El Haddad AA (1983a). Contribution to the lithostratigraphy of Miocene and Pliocene sediments of the Egyptian part of Red Sea coast. In: The 21st Annual Meeting of the Geological Society of Egypt (Abstracts), pp. 5-6.

Philobbos ER, El Haddad AA (1983b). Tectonic control on Neogene sedimentation along the Egyptian part of Red Sea coastal area. In: The 5th International Conference of Basement Tectonics, Cairo (Abstract).

Philobbos ER, El-Haddad AA, Mahran TM (1988). Comparison between Miocene and Pliocene facies distribution related to syn-rift tectonics along the Egyptian part of Red Sea coastal area. In: EGPC 9th Petroleum Exploration and Production Conference, pp. 246-254.

Philobbos ER, El-Haddad AA, Mahran TM (1989). Sedimentology of syn-rift Upper Miocene (?)-Pliocene sediments of the Red Sea area: a model from the environs of Marsa Alam, Egypt. Egyptian Journal of Geology 33: 201-227.

Philobbos ER, El-Haddad AA, Luger P, Bekir R, Mahran TM (1993). Syn-rift Miocene sedimentation around fault-blocks in the Abu Ghusun-Wadi El Gemal area, Egypt. In: Purser BH, Philobbos ER, editors. Geodynamics and Sedimentation of the Red Sea –Gulf of Aden Rift System. Cairo, Egypt: Geological Society of Egypt Special Publications, pp. 115-142.

Purser BH (1998). Syn-rift diagenesis of Middle Miocene carbonate platforms on the north-western Red Sea coast, Egypt. In: Purser BH, Bosence DWG, editors. Sedimentation and Tectonics of Rift Basins: Red Sea - Gulf of Aden. London, UK: Chapman and Hall, pp. 379-389.

Purser BH, Barrier C, Montenat C, Orzag-Sperber F, Ott d'Estevou P, Plaziat JC, Philobbos E (1998). Carbonate and siliciclastic sedimentation in an active tectonic setting: Miocene of the north-western Red Sea rift, Egypt. In: Purser BH, Bosence DWG, editors. Sedimentation and Tectonics of Rift Basins: Red Sea - Gulf of Aden. London, UK: Chapman and Hall, pp. 239-270.

Purser BH, Philobbos ER, Soliman M (1990). Sedimentation and rifting in the NW parts of the Red Sea: a review. Bull Soc Geol France 1: 371-384.

Purser BH, Soliman M, M'Rabet A (1987). Carbonate, evaporite, siliciclastic transitions in Quaternary rift sediments of the northwestern Red Sea. Sediment Geol 53: 247-277.

Qilong F, Qing H, Bergman K (2007). Dolomitization of the Middle Devonian Winnipegosis carbonates in south-central Saskatchewan, Canada. Sedimentology 53: 825-848.

Qing H, Bosence DW, Rose EP (2001). Dolomitization by penesaline sea water in Early Jurassic Peritidal platform carbonates, Gibraltar, western Mediterranean. Sedimentology 48: 153-163.

Randazzo AF, Cook DJ (1987). Characterization of dolomitic rocks from the coastal moxing zone of the Floridian aquifer, Florida, USA. Sediment Geol 54: 169-192.

Rosenbaum J, Sheppard SM (1986). An isotopic study of siderites, dolomites and ankerites at high temperatures. Geochim Cosmochim Acta 50: 1147-1150.

Samuel MD, Saleeb-Roufaiel GS (1977). Lithostratigraphic and petrographic analysis of the Neogene sediments at Abu Ghusun, Um Mahara, Red Sea coast, Egypt. Freiberger Forschungschefte, Beitrage Zur Lithologie 323: 46-56.

Schwarzacher W (2005). The stratification and cyclicity of the Dachstein limestone in Lofer, Leogane and Steinernes Meer (Northern Calcareous Alps, Austria). Sediment Geol 181: 93-106.

Shaaban M, Hanafy H, Rashed M (1997). Dolomitization of Middle Miocene buildups, Um Gheig area, Red Sea coast, Egypt. Carbonate Evaporite 12: 264.

Shukla V (1988). Sedimentology and geochemistry of a regional dolostone: correlation of trace elements with dolomite fabrics. In: Shukla V, Baker PA, editors. Sedimentology and Geochemistry of Dolostones. Tulsa, OK, USA: SEPM Special Publications, pp. 145-157.

Soreghan G, Engel M, Furley RA, Giles KA (2000). Tectonic controls on early dolomite in Pennsylvanian algal mounds of the western Orogrande Basin, New Mexico. In: AAPG Annual Meeting, Tulsa, USA (Abstracts), Article #90914.

Sun QS (1992). Skeletal aragonite dissolution from hypersaline sea water: a hypothesis. Sediment Geol 77: 249-257.

Swart PK, Cantrell DL, Westphal H, Handford R, Kendall CG (2005). Origin of dolomite in the Arab-D Reservoir from the Ghawar Field, Saudi Arabia: evidence from petrographic and geochemical constraints. J Sediment Res 75: 477-491.

Tarabili E (1966). General outline of epeirogenesis and sedimentation in the region between Safaga, Quseir and Southern part of Wadi Qena, Eastern Desert, Egypt. AAPG Bull 50: 1890-1898.

Teedumae A, Nestor H, Kallaste T (2004). Sedimentary cyclicity and dolomitization of the Raikkula Formation in the Nurma drill core (Silurian, Estonia). J Geol 53: 42-72.

Tucker ME (1993). Carbonate diagenesis and sequence stratigraphy. Sediment Rev 1: 51-72.

Tucker ME, Calvet F, Henton J, Marshall J, Spiro B (1991). Dolomitization related to sequence boundaries: the Triassic Muschelkalk Platforms of Eastern Spain. In: Bosellini A, Brandner B, Flugel E, Purser B, Schlager W, Tucker M, Zenger D, editors. Dolomieu Conference on Carbonate Platforms and Dolomitization (Abstracts), Italy, 12–17 September 1991, p. 275.

Tucker ME, Wright VP (1990). Carbonate Sedimentology. Oxford, UK: Blackwell.

Turhan A, Erdogan T, Muharrem S (2004). Water circulation near the mixed water and microbiologic activity of the Mesozoic dolomite sequence, an example from the central Taurus, Turkey. Carbonate Evaporate 19: 107-117.

Van den Hurk AM, Betzler C (1991). Dolomitization and carbonate stratal patterns as a response of sea level changes (Paleogene, south Pyrenean foreland basin, Esera, Cinca and Cinqeta Rivers, Huesca, Spain). In: Bosellini A, Brandner B, Flugel E, Purser B, Schlager W, Tucker M, Zenger D, editors. Dolomieu Conference on Carbonate Platforms and Dolomitization (Abstracts), Italy, 12–17 September 1991.

Veizer J (1983). Trace elements and isotopes in sedimentary carbonates. Rev Mineral Geochem 11: 265-299.

Veizer J, Lemieux J, Gibling M, Jim S (1978). Paleosalinity and dolomitization of a lower Paleozoic carbonate sequence, Somerset and Prince of Wales Islands, Arctic Canada. Can J Earth Sci 15: 1448-1461.

Velde B (1992). Introduction to Clay Minerals. London, UK: Chapman and Hall.

Warren J (2000): Dolomite: occurrence, evolution and economically important associations. Earth-Sci Rev 50: 1-81.

Zenger DH, Dunham JB (1988). Dolomitization of Siluro-Devonian limestones in a deep core (5,350M), Southeastern New Mexico. In: Shukla V, Baker PA, editors. Sedimentology and Geochemistry of Dolostones. Tulsa, OK, USA: SEPM Special Publications, pp. 171-173.

Zengzhao F, Yongsheng Z, Zhenku J (1998). Type, origin and reservoir characteristics of dolostones of the Ordovician Majiagou Group, Ordos, North China platform. Sediment Geol 118: 127-140.